American Journal of Botany 92(8): 1234–1255. 2005.

COMPARATIVE INFRUCTESCENCE MORPHOLOGY IN *LIQUIDAMBAR* (ALTINGIACEAE) AND ITS EVOLUTIONARY SIGNIFICANCE[1]

STEFANIE M. ICKERT-BOND,[2,3,5] KATHLEEN B. PIGG,[3] AND JUN WEN[2,4]

[2]Department of Botany, The Field Museum of Natural History, Chicago, Illinois 60605-2496 USA; [3]School of Life Sciences, Arizona State University, Tempe, Arizona 85287-4501 USA; and [4]Laboratory of Systematic and Evolutionary Botany and Herbarium, Institute of Botany, Chinese Academy of Sciences, Beijing 100093 People's Republic of China

The sweet gum genus *Liquidambar* (Altingiaceae) has two species in eastern Asia, one in eastern North America, and one in western Asia. Mature infructescences are studied to provide anatomical, morphological, and micromorphological details, some of which are newly recognized. Homology is suggested between extrafloral spinose processes of *L. formosana* and *L. acalycina*, braid-like ornamentation of *L. styraciflua*, and broad intercarpellate areas of *L. orientalis*. Morphology, position, number, and the presence of similar structures in the closely related Hamamelidaceae s.s. support their derivation from sterile flowers. Morphological cladistic analysis using 43 characters supports the monophyly of *Liquidambar* with *Altingia* as its sister. The *matK* analysis contrastingly places *Altingia* sister to the *L. acalycina–L. formosana* clade, rendering *Liquidambar* paraphyletic. Discordance between morphological and *matK* data sets may result from both different rates of morphological evolution and convergence. Several similarities between *Altingia* and *L. acalycina* are symplesiomorphic in the morphological cladistic analysis. *Microaltingia apocarpela*, from the Cretaceous of eastern North America, documents the earliest known fossil divergence within Altingiaceae. The Miocene *Liquidambar changii* of western North America is sister to a clade of extant *Liquidambar* species. Consideration of this fossil evidence reveals complex intercontinental biogeographic disjunctions in Altingiaceae.

Key words: Altingiaceae; biogeography; infructescence; *Liquidambar*; phylogeny.

The family Altingiaceae Horan., with its approximately 15 tree species and excellent fossil record, is an important model for understanding northern hemisphere biogeography. The most commonly known genus, *Liquidambar* L. (Altingiaceae), contains four intercontinentally disjunct species in the temperate zone of the northern hemisphere. Two species are in eastern Asia, one is in western Asia, and one is disjunct between eastern North America and from central Mexico to Belize (Fig. 1). These arborescent taxa have unisexual, capitate, globose, woody infructescences composed of 25–50 helically arranged, bilocular capsules that bear several viable seeds per fruit and many abortive seeds. *Liquidambar* has been the focus of several studies exploring the evolution of intercontinental biogeographic disjunctions in the north temperate zone (see review in Wen, 1999). Allozyme (Hoey and Parks, 1991, 1994) and phylogenetic analyses of molecular sequencing data (Shi et al., 1998; Li et al., 1997a, b; Li and Donoghue, 1999) suggest a sister species relationship between the North American *L. styraciflua* L. and the western Asian *L. orientalis* Mill. within the genus. This hypothesized relationship suggests an historical connection across the North Atlantic, rather than a Eurasian route. *Liquidambar orientalis* may have diverged from relatives of *L. styraciflua* of North America prior to the disruption of the North Atlantic land bridge, around 45 million years ago (mya) (Graham, 1999; Tiffney and Manchester, 2001).

Traditionally, *Liquidambar*, *Altingia* Noronha, and *Semiliquidambar* Hung T. Chang have been treated as a subfamily of the Hamamelidaceae, as either the Altingioideae (Williams, 1855; Reinsch, 1890; Chang, 1979; Cronquist, 1981; Endress, 1989a; Qui et al., 1998; Li and Donoghue, 1999) or (incorrectly) as Liquidambaroideae (Harms, 1930; Bogle, 1986; Ferguson, 1989). Some authors have elevated the subfamily to family status as the Altingiaceae (Blume, 1828; Wilson, 1905; Chang, 1959; Rao, 1974), a taxonomic level accepted today by many (e.g., Judd et al., 2002; APG II, 2003).

The systematic composition of the Altingiaceae has been relatively stable, while its systematic position has been in flux. Traditionally, Hamamelidaceae s.l. (including Altingiaceae) has been considered a member of the Hamamelididae Takht. (Cronquist, 1981). Recent molecular studies have shown this assemblage to be polyphyletic and support Altingiaceae and Hamamelidaceae s.s. as members of the saxifragoid clade within a larger rosid clade (Chase et al., 1993; Magallón et al., 1999; Soltis et al., 2000; APG II, 2003). In an alternative classification, the order Altingiales, including Altingiaceae and Rhodoleiaceae, was recognized and included in the superorder Trochodendranae along with the order Trochodendrales (Doweld, 1998). Recognition of the four species of *Liquidambar* has been widely accepted; however, a few authors have suggested that *L. styraciflua* and *L. orientalis* might be conspecific based on the continuous, clinal variation among leaves and on

[1] Manuscript received 10 November 2004; revision accepted 16 May 2005.

The authors thank A. Linn Bogle (NHA), Charlotte M. Christy (Augusta State University, Augusta, Georgia), Randall C. Hitchin (Washington Park Arboretum, Seattle, Washington), Donald J. Pinkava (ASU), S. Shi (SYS), and Emily Wood (GH) for providing material for study; B. Chen (IBSC), Y. W. Lam (HK), Phan Ke Loc (HNU), P. Wan (HK), and K. Y. Yip (HK) for assistance in the field; the curators of the following herbaria for allowing access to collections: A, ASU, E, F, FI, GH, HK, HN, IBSC, K, MO, P, PE, and XAL; Zorica Dabich (F) for providing illustrations; and Tingshuang Yi (F) for Chinese translations. This study was funded by a Boyd Postdoctoral Fellowship, the Field Museum of Natural History; National Geographic Society Explorers Grant NGS-7644-04; a grant from the Field Dreams Program, Women's Board, Field Museum of Natural History; and a generous donation by the Wallace Desert Gardens, Scottsdale, Arizona, to S. M. I.-B.; National Science Foundation EAR-9980388 and EAR-0345838, and a Minigrant, College of Liberal Arts and Sciences (CLAS), Arizona State University, to K. B. P.; and National Science Foundation DEB-0108536; and an Overseas Chinese Collaborative Research grant from the Chinese Academy of Sciences, to J. W.

[5] E-mail: sbond@fieldmuseum.org.

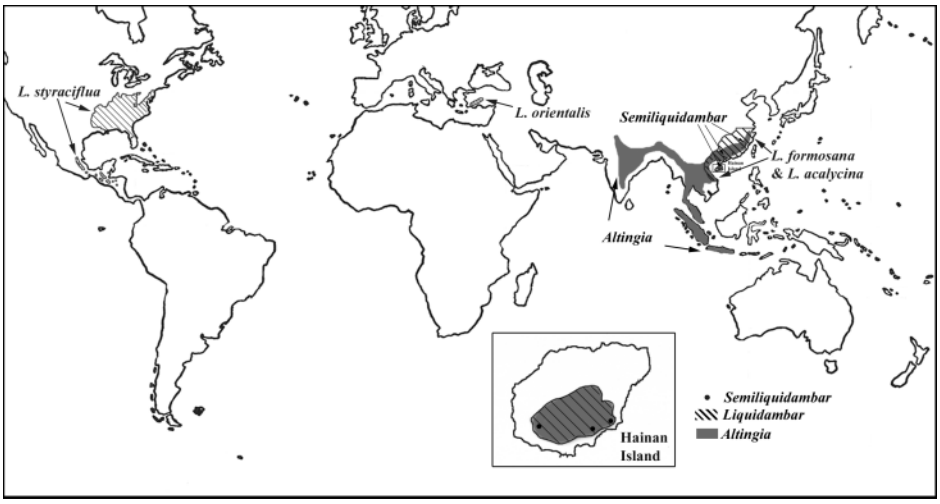

Fig. 1. Distribution map for genera of Altingiaceae, based mainly on Chang (1962), Little (1971), Wood (1972), Boratynska (1984), and Efe (1987). *Liquidambar formosana* and *L. acalycina* have the same geographic areas in China.

the relatively subtle morphological differences between their infructescences (Reichinger, 1943; Meikle, 1977; Ferguson, 1989). The similarity between these two species may also be due to morphological stasis that is thought to occur among many temperate intercontinental disjunct genera (Wen, 1999). Stasis is supported by the morphological similarities in the two species, despite their high level of molecular divergence (Wen, 1998, 1999, 2001). Morphological stasis has also been proposed for other disjunct genera including *Liriodendron* L. (Parks and Wendel, 1990), and *Magnolia* L. sect. *Rytidospermum* (Qui et al., 1995). We now know that a fossil species of *Liquidambar* sharing many similarities with the extant Asian species *L. acalycina* was present by the middle Miocene (15 mya) (Pigg et al., 2004), suggesting that an earlier migration of ancestors of *L. styraciflua* and *L. orientalis* is realistic.

In the present study we describe comprehensive details of infructescence morphology, micromorphology, and anatomical structure of the four extant species of *Liquidambar*. This study was undertaken to better understand the overall morphological diversity, character evolution, and delimitation of extant species within the genus, and the biogeographic implications of these characters. Detailed comparable analyses of the other two genera of Altingiaceae, *Altingia* and *Semiliquidambar*, and of related fossil taxa, are currently underway within a broader study to detail the phylogeny, morphological diversification, evolutionary history, and biogeography of the Altingiaceae.

MATERIALS AND METHODS

Taxa for study were obtained by fresh or herbarium sample and photographed for general features (Appendix). Measurements given are the mean of 10 individuals counted (Table 1). Specimens for anatomical sections were prepared using standard histological techniques that included embedding in Paraplast Plus tissue embedding medium (Monoject Scientific, St. Louis, Missouri, USA) and sectioning on a rotary microtome at 20 μm thick. Mature infructescences were softened with ethylene diamine prior to embedding (Carlquist, 1982). For anatomical studies, dry seeds were rehydrated for 7 d in equal parts of glycerol, water, and ethanol and then sectioned by hand (Lobova et al., 2003). Seeds and carpel wall surfaces were prepared for scanning electron microscopy by sputter coating and scanned with an Amray 1400 and Amray 1810 SEM (KLA Tencor, Bedford, Massachusetts, USA). Except where noted, terminology follows that of Bogle (1986).

To evaluate the morphological evolution of taxa in *Liquidambar* and its close relatives, we undertook a morphological cladistic analysis. We scored all potentially informative morphological variations observed for the four species of *Liquidambar*, *Altingia chinensis*, and two recently described fossil taxa, the Cretaceous *Microaltingia apocarpela* Zhou, Crepet and Nixon from eastern North America (Zhou et al., 2001), and the middle Miocene, *Liquidambar changii* Pigg, Ickert-Bond & Wen from western North America (Pigg et al., 2004). The Altingiaceae have occupied an isolated position in the saxifragoid clade, which makes outgroup selection difficult. *Exbucklandia* R. W. Brown and *Hamamelis* L. of Hamamelidaceae s.s. (also in the saxifragoid clade) were selected as the outgroups in our analysis following earlier suggestions (Table 3). *Semiliquidambar* was not included in the analysis because it has been hypothesized to be an intergeneric hybrid (Bogle, 1986; Ferguson, 1989). We emphasized reproductive structures and expanded the established morphological matrix of Hufford (1992), and also included the characters of chromosome number and iridoid chemistry. Forty-two characters were selected on the basis of interspecific variations among the sampled taxa (Table 3). They consist of 38 binary and four multistate characters. All multistate characters were treated as unordered. Quantitative characters were coded following simple gap coding (Archie, 1985). Characters for which discrete states could not be recognized (i.e., continuous characters) were excluded from the data matrix. Data are mainly derived from our own observations and partly from the literature (Chang, 1962; Melikian, 1973; Kaul and Kapil, 1974; Goldblatt and Endress, 1977; Bogle, 1986; Endress, 1989a, b, c; Ferguson, 1989; Hufford and Endress, 1989; Hufford and Crane, 1989; Endress and Stumpf, 1990; Hufford, 1992). An annotated list of all characters is presented in Table 2 and the morphological matrix is presented in Table 3.

Parsimony analysis was performed using a branch-and-bound search with MULPARS and furthest addition sequence options in PAUP* (version 4.0b10; Swofford, 2002). Character states were coded as unordered and all characters were weighted equally. The amount of support for monophyletic groups revealed in the maximally parsimonious tree(s) (MPTs) was examined with 1000 bootstrap replicates (Felsenstein, 1985) with the random addition and the heuristic search options.

We used *matK* sequences generated from a recently published phylogenetic study of Altingiaceae (Shi et al., 2001) as a molecular framework for discussing our morphological evolution in *Liquidambar* and close relatives. Our preliminary results from analysis of waxy and *trnL-trnF* generated the same topology for these taxa as in the *mat*K tree (Ickert-Bond et al., 2004). For the *matK* data set, we obtained the sequence data from GenBank: *Liquidambar styraciflua* (AF133219), *L. acalycina* Hung T. Chang (AF133222), *L. formosana* Hance (AF015650), *L. orientalis* (AF133220), *A. chinensis* (AF133225), *Exbucklandia populnea* (AF128831), and *Hamamelis virginiana* (AF013046).

TABLE 1. Comparison of characters measured within *Liquidambar*. All measurements are in millimeters (means are in parentheses).

Character		Character			
		L. acalycina	*L. formosana*	*L. orientalis*	*L. styraciflua*
Infructescence	Length (L)	14.45–29.93 (26.96)	24.31–31.28 (27.24)	12.20–26.62 (17.92)	19.00–34.62 (30.34)
	Width (W)	18.40–31.07 (26.92)	22.49–30.40 (27.01)	14.45–26.96 (17.43)	20.25–40.87 (31.60)
	L/W ratio	0.77–1.23:1 (1.01:1)	0.89–1.14:1 (1.01:1)	0.78–1.08 (0.90:1)	0.84–1.09 (0.97:1)
	No. of fruits/infructescence	17–26	32–37	33–48	34–40
	Peduncle length	53.17–65.92 (59.75)	38.94–63.05 (55.16)	13.98–47.48 (29.89)	36.71–55.89 (42.75)
	Peduncle width	0.93–1.29 (1.10)	1.19–1.53 (1.38)	0.88–1.45 (1.20)	0.73–1.10 (0.95)
	Extra floral structures	Spines, short	Spines, long	Smooth rim	Bumpy rim
Style	Orientation	Curved	Coiled	Curved	Curved
	Length	4.01–6.42 (5.50)	6.79–9.75 (8.24)	2.13–3.51 (2.95)	4.18–6.28 (5.18)
Carpel	Length	6.12–9.98 (8.01)	8.06–9.40 (8.73)	5.81–6.21 (6.01)	12.05–12.70 (12.36)
	Width	2.58–3.16 (2.79)	2.18–2.19 (2.19)	2.27–2.77 (2.52)	4.21–4.56 (4.34)
	L/W ratio	2.37–3.16:1 (2.87:1)	3.70–4.29:1 (3.99:1)	2.10–2.74:1 (2.38:1)	2.79–2.91:1 (2.85:1)
Seed	Length	4.86–6.90 (5.77)	7.06–8.20 (7.71)	4.55–4.85 (4.73)	7.79–8.51 (7.98)
	Width	2.84–3.73 (3.16)	1.69–2.13 (1.93)	1.82–1.87 (1.85)	1.86–2.79 (2.33)
	L/W ratio	1.67–2.04:1 (1.83:1)	3.65–4.46:1 (4.0:1)	2.43–2.66:1 (2.55:1)	2.90–4.24:1 (3.43:1)
	Wing	Circular	Distal	Distal	Distal
	Seed coat surface pattern	Polygonal	Rectangular	Rectangular	Rectangular
	Epidermal cells in cross-section	Tabular	Cuboidal	Cuboidal	Cuboidal
	No. of rows of sclereids	1	2–3	1–2	1–2

We executed the phylogenetic analysis with both parsimony and Bayesian methods. Base frequencies were empirically determined, and the transition: transversion (K) ratio and gamma shape parameter (Γ) were estimated on MP trees under the model of sequence evolution, chosen using results from ModelTest version 3.06 (Posada and Crandall, 1998). Bayesian inference was conducted using MrBayes version 3.0 (Huelsenbeck and Ronquist, 2001). The Markov chain Monte Carlo algorithm (MCMC) was run for 2 000 000 generations with four incrementally heated chains, starting from random trees and sampling one out of every 100 generations. A majority-rule consensus tree was calculated with PAUP* from the last 18 001 out of the 20 001 trees sampled. The first 2000 trees (burn-in) were excluded to avoid trees that might have been sampled prior to convergence of the Markov chains. The posterior probability of each topological bipartition was estimated by the frequency of these bipartitions across all 18 001 trees sampled. Internodes with posterior probabilities $\geq$95% were considered statistically significant.

The relationships of the morphological analysis were tested against alternative hypotheses. Trees with topological constraints were constructed using MacClade 4.03 (Maddison and Maddison, 2000), then loaded into PAUP*. Heuristic searches were conducted to find the shortest trees consistent with each imposed constraint. The following three hypotheses were tested: (1) monophyly of *Liquidambar acalycina* and *L. formosana*; (2) *matK* phylogeny; and (3) monophyly of the eastern Asian *Altingia chinensis*, *L. acalycina*, and *L. formosana*. The additional steps required for a particular constraint are given by the difference in length between the shortest trees obtained for the constrained versus unconstrained tree.

We employed the partition homogeneity test (Farris et al., 1995) and the Templeton's test (Templeton, 1983) to evaluate the congruence of the morphological and molecular data sets. The partition homogeneity test was conducted with PAUP* with 100 replicates of heuristic search using TBR branch-swapping and gaps treated as missing data. Topological congruence between the gene trees was evaluated with the Templeton's test, as implemented in PAUP*.

RESULTS

Morphological description—*General features*—The pistillate reproductive structures in *Liquidambar* are characterized by a spherical inflorescence (Figs. 2C, 4B, 5B, 6B) that develops into a persistent, woody infructescence (Figs. 2A, 3A, 4A, 5A, E, 6A). It is composed of closely spaced, multiple (~25–50) bilocular fruits that appear to be helically arranged around a central axis borne on an elongate peduncle. Extrafloral structures that have been variably interpreted are found within the infructescence head. Depending on the species under study they include, variously, elongate, spine-like processes (*L. acalycina*, *L. formosana*, Figs. 3B, 4C), thickenings that appear organized into a tangentially elongate ''braided'' structure along the hypanthial surface (*L. styraciflua*, Figs. 2A, 6D), or smooth, slightly thickened areas between adjacent fruits (the ''peripheral rim'' sensu Gregor, 1978 of *L. orientalis*; Ferguson, 1989; Fig. 5E).

Styles found on inflorescences are elongate, sometimes curved or even coiled, with broad stigmatic surfaces (Figs. 2B, 4D, 5B, F, I, 6B, E). Although the stigmatic surfaces are not always persistent, the styles typically become sclerified and can be found on mature infructescences (Figs. 3A, B, 5E, 6D). Stamens producing mature polyporate pollen characteristic of the genus are typically grouped into separate staminate inflorescences; however, it is fairly common to find several individual stamens with mature pollen developed within a pistillate inflorescence (Figs. 2C, 6K, arrows).

The bilocular fruits are wedge- to spindle-shaped, fused basally, and free distally (Figs. 2B, 4C, 6I). In some taxa, individual fruits are tightly connected to one another, resulting in a cohesive infructescence (Figs. 4E, 5D, 6H); in others, they are only loosely attached to one another, and the infructescence falls apart into individual fruits upon hand-sectioning (Fig. 3C). Carpels are fused basally along their ventral margins. In this region the tissues typically become thickened and sclerified (Figs. 2E, 3D, F, 4F).

Fruits typically have a two-zoned pericarp consisting of a persistent inner carpel wall of palisade-like cells one to several cells thick (Figs. 2E, H, 3H, 4H, 5M, 6G) and an outer pericarp 20–30 cells thick (Fig. 2E, F). The inner palisade cells sometimes have thickened walls (Fig. 6G). To the outside of the palisade layer, the outer pericarp is made of approximately

TABLE 2. Morphological characters and character states[a].

Characters	State
Vegetative morphology	
Leaf architecture (1–4)	
1. Texture	chartaceous (0), coriaceous (1)
2. Lamina, length/width ratio	>3:1 (0), <2:1 (1)
3. Shape	entire (0), lobed (1)
4. Venation	pinnate (0), palmate (1) (modified from H-6 of Hufford, 1992)
Leaf anatomy (5–6)	
5. Stipules	absent (0); present, <5 mm (0), present, >10 mm (1) (Chang 1962)
6. Stomatal opening shape	elongate, thin (0), short, broad (1) (Ferguson, 1989)
Reproductive morphology	
General floral morphology (7–10)	
7. Plant sex distribution	bisexual (0), monoecious (1), H-21
8. Nectary	present (0), absent (1) (modified from H-27 of Hufford, 1992)
9. Perianth parts	present (0), absent (1) (Kaul and Kapil, 1974)
10. Extrafloral processes	absent (0), tubercles, knob-like, or fused (1), spinose elongated structures (2)
Androecium morphology (11–14)	
11. Anthers	with dorsal pollen sacs reduced (0), tetrasporangiate (1) (Endress and Stumpf, 1990)
12. Anther theca length/filament length	<1 (0), >1 (1) (Chang, 1962; Hufford and Crane, 1989)[b]
13. Thecae with broad block-like shoulders	absent (0), present (1) (Hufford and Endress, 1989)
14. Stomia bifurcating at proximal and distal ends	present (0), absent (1) (Hufford and Endress, 1989)
Pollen morphology (15–19)	
15. Pollen	tricolpate (0), polyporate (1) (Hufford and Crane, 1989)
16. Pollen size	<25 μm (0), >35 μm (1) (Hufford and Crane, 1989). Most taxa have pollen grains larger than 35 μm, while those of the outgroup taxa are generally smaller than 25 μm (Chang, 1964)
17. Aperture L/W ratio	>3:1 (0), 1:1 (1), (modified from H-53 of Hufford, 1992)
18. Ectoaperture termini	rounded (0), pointed (1) (modified from H-54 of Hufford, 1992)
19. Secondary sculpture of tectum	smooth (0), papillate (1) (Hufford and Crane, 1989)
Gynoecium morphology: carpel characters (20–36)	
20. Carpel shape	square (0), wedge-shaped (1), elliptical (2)
21. Styles	persistent (0), ephemeral (1)
22. Styles	angled (0), straight (1) (Chang, 1962)
23. Style tips	recurved (0), coiled (1).
24. Styles	narrow (0), thick (1).
25. Multicellular stigmatic hairs	absent (0), present (1) (Endress, 1989b).
26. Inner carpel wall (palisade) wall thickening	absent (0), present (1).
27. Inner carpel wall surface pattern of cells	elongate (0), broad (1).
28. Inner carpel wall layers	two to multi-layered (0), single-layered (1).
29. Ovules per carpel	strictly 1 (0), 5–8 (1), many, >10 (2), H–39 (Bogle, 1986; Endress, 1989b).
30. Fruits with an explosive (ballistic) ejecting mechanism	present (0), absent (1) (Endress, 1989b, Tiffney, 1986).
31. Infructescence size	<1.0 cm (0), 1–2 cm (1), >2.5 cm (2) (Table 2; Efe, 1987).
32. Number of fruits per infructescence	mostly one (0), 3–9 (1), >20–37 (2), >45 (3).
33. Anthers developed in pistillate infructescence	absent (0), present (1).
34. Peduncle length	up to 1.5 cm (0), >2 cm (1).
35. Fruits exserted	absent (0), present (1).
36. Fruits attached to one another	loosely (0), tightly (1).
Seed morphology (37–40)	
37. Seed with wing	absent (0), lateral flange (1), distal wing (2)
38. Seed viability	seeds mostly fertile (0), fertile and sterile seeds (1).
39. Seed coat	thick, >10 layers of sclereids (0), thin, <4 layers of sclereids (1) (Melikian, 1973; Hufford and Crane, 1989).
40. Seed coat micromorphology, cell shape	broad, polygonal (0), elongate, rectangular (1).
Chemistry (41)	
41. Iridoids	(0) absent; (1) present. H-46.
Chromosome number (42)	
42. Chromosome number	n = 12 (0), n = 16 (1), n = 32 (2) (Endress, 1989c; Goldblatt and Endress, 1977).

[a] H-X = character number X in Hufford (1992), with states not found in this data set eliminated. All characters are unordered.

[b] In the outgroup taxa, the filaments are much shorter than the anther and the anthers are almost sessile, in *Liquidambar* filaments are almost twice as long as the anthers.

TABLE 3. Data matrix for *Liquidambar*, *Altingia*, and outgroups. See Table 2 for character traits for the numbers in the matrix.

Taxon	Character number																				
	1	2	3	4	5	6	7	8	9	10	11	12	13	14	15	16	17	18	19	20	21
Hamamelis virginiana	0	0	0	0	0	—	0	0	0	0	0	0	0	0	0	0	1	0	0	0	0
Exbucklandia populnea	0	1	1	1	2	—	0	—	1	0	0	0	0	0	0	0	1	0	0	0	1
Microaltigia apocarpela	—	—	—	—	—	—	0	—	0	—	—	—	—	—	—	—	—	0	0	1	1
Liquidambar changii	—	—	—	—	—	—	—	—	1	1	—	—	—	—	—	—	—	—	—	1	0
Altingia chinensis	1	0	0	0	1	0	1	1	1	1	1	0	1	0	1	1	0	1	1	1	1
Liquidambar acalycina	0	1	1	1	2	0	1	1	1	2	1	1	0	1	1	1	0	1	1	1	0
Liquidambar formosana	0	1	1	1	2	0	1	1	1	2	1	1	0	1	1	1	0	1	1	2	0
Liquidambar orientalis	0	1	1	1	2	1	1	1	1	1	1	1	0	1	1	1	0	1	1	2	0
Liquidambar styraciflua	0	1	1	1	2	1	1	1	1	1	1	1	0	1	1	1	0	1	1	2	0

Note: — denotes missing data, since these characters were not available from the fossil taxa or the outgroup.

four layers of ground tissue and a uniseriate epidermis. The outer pericarp's innermost layer is a zone of 5–6 cells thick of tangentially elongate parenchyma cells (Figs. 2F, G, 3H, J). The second layer is an area of larger parenchymatous cells, 2–4 cells thick, which contains resin canals (Figs. 2F, 3J, 5M). This layer is often disrupted and often breaks down in mature fruits (Figs. 2G, 3F, 4F). Next are the vascular strands comprised of 2–5 primary xylem elements and 2–6 layers of phloem, surrounded by often fibrous bundle sheaths (Figs. 2 E, I, 5L). The outermost ground tissue is composed of 8–10 layers of parenchymatous cells, within which resin canals and crystals are found (Fig. 4L). A uniseriate epidermis is composed of tabular to radially elongate to papillate cells (Figs. 2E, 4K).

Infructescences are borne on a woody peduncle of varying length. The axis ranges from 0.9–2.0 mm in diameter with a central stele (1.1 mm in diameter) surrounding a broad pith and contains a small amount of secondary tissue surrounded by ground tissue that contains prominent resin canals (Fig. 2H). The stele extends into the central part of the infructescence where it appears as individual sympodia, each subtended by several rows of secondary tissues (Fig. 2H).

A large number of anatropous ovules are initially borne broadly in a vertical row along the ventral margins of each carpel (Figs. 2C, E, 6I). Typically, only a few ovules develop into mature seeds, and they tend to be found basally, closest to the central axis. Maturing seeds are either broadly obovate with a circular flange (Fig. 3K, L) or elongate to spindle-shaped with a prominent distal wing (Figs. 4M, 5C, 6F, 8A–D). They are typically speckled or striped and there is a wide variation in this feature, even within a single infructescence. The seed coat is several layers of cells thick, with a prominent outer layer of palisade cells and around 3–5 inner layers surrounding a straight embryo cavity. Numerous abortive seeds are variable in shape and have a prominent palisade layer that resembles the outermost seed coat of mature seeds, but otherwise they fail to develop.

Liquidambar acalycina (Figs. 2I, 3A–L, 7A, G, 8A, E, 9A, E, K)—Infructescences are spherical with persistent, prominent curved styles and additional spinose extrafloral structures (Fig. 3A, B) and measure 14.5–30.0 (X = 27.0) mm high by 18.4–31.1 (X = 26.9) mm wide, with a length/width (L/W) ratio ranging from 0.8–1.2: 1 (= 1.0 : 1). Peduncles are 53.2–65.9 (X = 59.8 mm) long by 0.9–1.3 (X = 1.1) mm wide. Each infructescence is made of ~26 individual bilocular fruits that appear to be helically arranged on a central axis.

The persistent styles are ~4.0–6.5 (X = 5.5) mm long and curving. The paired styles from each fruit curve toward one another at their tips (Fig. 3A, B). They gradually extend basally into elongate, triangular-shaped bases that expand to ~3.4 mm wide. Surrounding each fruit are typically 10–12 short, spinose extrafloral structures, each up to ~2.7 mm long × ~0.3 mm wide that are attached to a wider cushion-like base ~0.9 mm across (Fig. 3B). Both the styles and extrafloral structures are finely striated vertically.

Fruits are 8.0 mm long × 2.8 mm wide (L/W ratio of 2.9 : 1), wedge-shaped and fused for ~2/3–3/4 of their total length, and free distally (Fig. 3C, D). Fruits are held together somewhat loosely (Fig. 3C), with a relatively thin pericarp, and spaces appear between adjacent fruits (Fig. 3E, F). In mature infructescences the pericarp is composed of an inner palisade layer two cells thick lining the locule (Fig. 3H), and a multicellular outer fruit wall (Fig. 3J). The palisade layer has two rows of radially elongate, thin-walled cells with individual cells ranging in size from 8–9 μm long × 2–11 μm wide (Fig. 3H). The outer fruit tissue is typically torn in mature infructescences, with some of the innermost layers adhering to the inner palisade layer (Fig. 3F). To the outside of the carpel lining, the next layer is a single layer of tabular cells that are slightly tangentially elongate and 8 μm long × 2 μm wide (Fig. 3F, H). To the outside is a zone of tangentially elongate cells around 6–8 cells thick (Fig. 3H). A zone 12–20 cells thick of more isodiametric cells makes up the central fruit tissue, with the outermost tissues containing vascular bundles subtended by prominent resin canals (Fig. 3J) and fiber bundles 5 μm wide that subtend the vascular bundles (Fig. 3J). The surface of the inner carpel wall has tangentially elongate cells, that appear rod-like and anastomosing (Fig. 7G).

Seeds are 5.8 mm long × 4.7 mm wide (L : W ratio, 1.8 : 1) with a circular flange surrounding the central body, resulting in a somewhat triangular appearance (Figs. 3K, L, 9A). Cells of the seed coat are polygonal (4–5 sided) and slightly elongate, and appear slightly thickened on the anticlinal walls (Fig. 8E). The cuticle of the epidermis is thin and epidermal cells are tabular in cross-section (Fig. 9J). Below the epidermis is a layer of fibers with large lumina (Fig. 9E), followed by crushed epidermal cells of the inner integument. To the inside of this layer are parenchymatous cells of the endosperm (Fig. 9E). The embryo is straight (Fig. 9A).

The most distinctive features of this species are the paired, curved styles and spinose extrafloral structures (Fig. 3B), the loosely attached fruits (Fig. 3C), the prominent basal pad of tissue in the fruits (Fig. 3D), and the triangular, flanged seeds (Fig. 3K, L) with a polygonal seed coat pattern (Fig. 8E) composed of epidermal cells that are tabular in cross-section (Fig. 9J).

TABLE 3. Extended.

Character																				
22	23	24	25	26	27	28	29	30	31	32	33	34	35	36	37	38	39	40	41	42
0	0	0	0	—	—	—	0	0	1	0	0	0	0	0	0	0	0	—	0	0
0	0	0	0	—	—	—	1	1	1	1	0	0	0	0	0	0	1	—	0	2
—	—	—	—	—	—	—	2	—	0	1	—	—	—	—	0	—	—	—	—	—
1	0	0	—	—	0	—	2	1	2	2	1	1	1	0	2	1	1	0	—	—
0	0	0	0	0	0	0	2	1	2	2	1	1	0	0	2	1	1	0	1	1
1	0	0	1	0	0	1	2	1	2	2	0	1	1	0	2	1	1	0	1	1
1	1	0	1	0	1	1	2	1	2	2	0	1	1	1	1	1	1	1	1	1
1	0	1	1	1	1	1	2	1	1	3	0	1	1	1	1	1	1	1	1	1
1	0	1	1	1	1	1	2	1	2	2	0	1	1	1	1	1	1	1	1	1

Liquidambar formosana (Figs. 2F, 4A–M, 7B, H, 8B, F, 9B, F)—Infructescences are spherical with persistent styles (Fig. 4A) and measure 24.3–31.0 (X = 27.2) mm high by 22.5–30.4 (X = 27.0) mm wide, with a L/W ratio ranging from 0.9–1.1 : 1 (X = 1.0 : 1). Peduncles are 38.9–63.1 (X = 55.2) mm long × 1.2–1.5 (X = 1.4) mm wide. Each infructescence is made up of ~34 individual bilocular fruits that appear to be helically arranged on a central axis.

Styles are 6.8–9.8 (X = 8.2) mm long. When found in inflorescences, they have tightly coiled tips that resemble fern croziers or ''fiddleheads'' (Fig. 4D); at maturity within infructescences they become somewhat dried and brittle and slightly uncoiled, but remain tightly coiled at the very tip (Fig. 4C). Styles extend basally into abruptly broad bases that expand to ~2.7 mm wide (Fig. 4C, I). Surrounding each is a group of around a dozen spinose extrafloral structures up to ~6.9 mm long × ~0.3 mm wide that resemble the styles except for lacking the coiled tips and stigmatic areas (Fig. 4C). These extrafloral structures each expand basally into a triangular base ~1.5 mm across. They are fused together basally into elongate cylinders up to ~8.5 mm long that greatly resemble the paired ovaries of each fruit (Fig. 4C). These structures are further fused together to form a band that surrounds a viable fruit (Fig. 4C).

Fruits are 8.7 mm long × 2. 2 mm wide (L/W ratio, 4 : 1), cylindrical to spindle-shaped, fused for ~3/4 of their total length and free distally (Fig. 4E). Fruits are held together tightly and have relatively thin fruit walls (Fig 4E). The fruit wall is composed of an inner, uniseriate palisade layer (Fig. 4F, G, H) and an outer pericarp (Fig. 4K, L). Individual cells of the inner palisade layer are radially elongate with thin walls that may have obliquely oriented rather than entirely perpendicular end walls (Fig. 4H). Palisade cells range in size from 26–28 μm long × 6–14 μm wide. To the outside, a remnant of the outer pericarp adheres to the palisade layer (Fig. 4H). The organization of the outer fruit wall is similar to the general structures described earlier for *L. styraciflua* (Fig. 2G) and *L. acalycina*. Distinctive features of the pericarp in this species include numerous druse crystals in the outermost pericarp and epidermal cells that are extremely elongate radially (Figs. 2F, 4K, L). Surface features of the inner carpel wall have short cells, that appear slightly raised above the general surface (Fig. 7G).

Seeds are 7.7 mm long × 1.9 mm wide (L/W ratio, 4.0 : 1) and very tapered, flattened in transverse section (Fig. 4G), and have a prominent distal wing that may be up to 3.8 mm long (Figs. 4M, 8B). Embryos found within seeds (Fig. 4G) are straight. Cells of the seed coat are tangentially elongated and rectangular with relatively thickened anticlinal walls in surface view (Fig. 8F). Epidermal cells of the seed coat are rectangular in cross-section and are covered by a thin cuticle. To the inside of the epidermis is a hypodermal layer that contains druse crystals, which in turn is followed by the outer integument of mostly crushed parenchyma cells. To the inside of the hypodermis are 2–3 layers of macrosclereids with small lumina (Fig. 9F), followed by the inner integument and the multilayered parenchymatous endosperm (Fig. 9F).

Features that are of particular diagnostic value for this species include the prominent extrafloral structures, the highly coiled style tips, the presence of druses in the outer fruit wall, the elongate seeds with a prominent distal wing (Fig. 4M), and 2–3 layers of macrosclereids in the seed coat (Fig. 9F).

Liquidambar orientalis (Figs. 5A–M, 7C, I, 8C, G, 9C, G, I)—Infructescences are spherical with persistent styles (Fig. 5A, E), and a broad, relatively smooth surface between adjacent fruits (Fig. 5E) and measure 12.2–26.6 (X = 14.9) mm high by 14.5–27.0 (X = 17.4) mm wide, with a L/W ratio ranging from 0.8–1.1 : 1 (X = 0.9 : 1). Peduncles are 14.0–47.5 (X = 29.0) mm long × 0.9–1.5 (X = 1.2) mm wide. Each infructescence is made up of ~48 individual bilocular fruits that appear to be helically arranged on a central axis.

Styles are 2.1–3.5 (X = 3.0) mm long. When found in inflorescences, styles are thick and fleshy, with a simple beak-like stigmatic tip (Fig. 5G). In mature infructescences, styles are persistent, with each attached to an elongate, triangular base up to ~3.1 mm wide. They are somewhat vertically striated and may frequently be broken at the tip (Fig. 5E).

Fruits are 6.0 mm long × 2.5 mm wide (L/W ratio 2.4 : 1), cylindrical to slightly wedge-shaped (Fig. 5C), and fused for ~2/3 to 3/4 of their total length and free distally. Fruits are held together fairly tightly, with relatively thin fruit walls. The fruit wall is composed of an inner palisade layer (Fig. 5K, M) and an outer pericarp (Fig. 5L). The palisade layer is a single cell thick. Individual cells are cuboidal to slightly radially elongate with thickened walls and range from 10–11 μm long × 3–5 μm wide (Fig. 5J). Surface features of the inner carpel wall show short, rectangular cells, with oblique end walls (Fig. 7I).

Seeds are 4.7 mm long × 1.9 mm wide (L/W ratio 2.6 : 1), elongate, and have a relatively short distal wing (Fig. 5C). The seed body is often irregular in shape, sometimes with a deep elongate groove (Fig. 5C). Cells of the seed coat are tangentially elongate, rectangular with thickened anticlinal walls, and oblique end walls (Fig. 8G). The epidermal cells are cuboidal in cross-section and are covered by a thick cuticle (Fig. 9G). Below the epidermis is a single-layered hypodermis containing druse crystals (Fig. 9I), followed by 2–3 layers of macro-

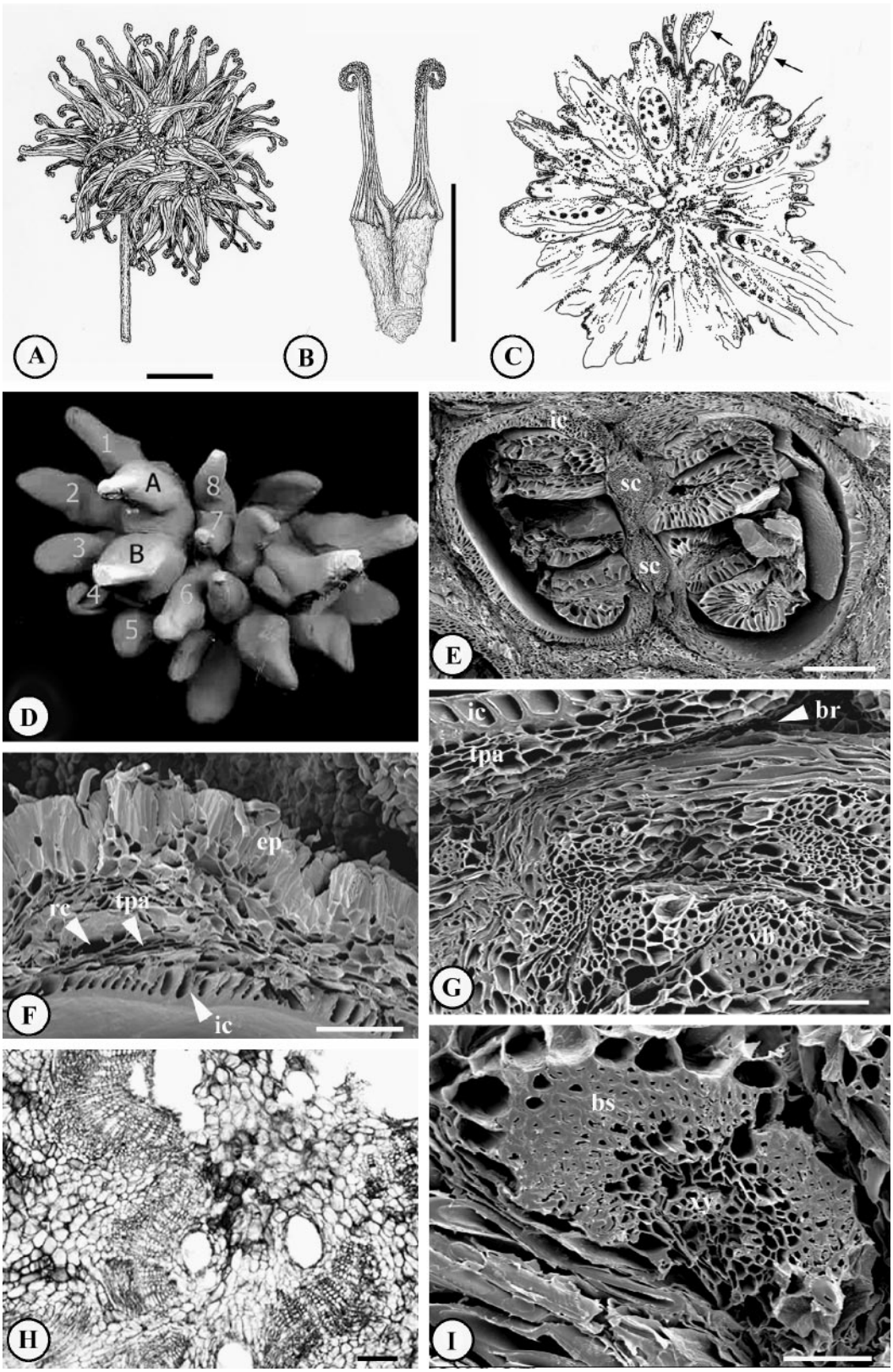

Fig. 2A–H. General features of *Liquidambar* infructescences. A–C, G–H. *L. styraciflua*. E–F. *L. formosana*. I. *L. acalycina*. **A.** Diagram of mature infructescence with persistent styles, style bases, and braided ornamentation. **B.** Diagram of bilocular fruit showing fusion below, but apocarpy distally. **C.** Diagram of cross-section showing bilocular fruits and occasional stamens (at arrows) interspersed between adjacent fruits. **D.** Clay model of infructescence showing developing bilocular fruit (A–B) and extrafloral processes (1–8). **E.** SEM of cross-section of bilocular fruit showing inner carpel wall and areas of fusion along ventral margin with central thickened patches of sclerenchyma. **F.** SEM of cross-section of pericarp showing outer epidermis, larger parenchyma cells with

sclereids each with a small lumen (Fig. 9G). To the inside is the epidermis of the outer integument, followed by parenchymatous cells of the endosperm.

Characteristic features of this species include the thick, relatively smooth areas between individual fruits, the cylindrical to spindle-shaped carpels, relatively short styles, the large number of flowers per inflorescence and the elongate seeds with deep grooves and relatively short distal wings, a mulicellular layer of macrosclereids in the seed coat (Fig. 9G), and thickened anticlinal walls of the inner carpel wall.

Liquidambar styraciflua (Figs. 6A–N, 7D–F, J, 8D, H, 9D, H)—Infructescences are spherical with persistent styles and small knob-like protuberances on surfaces (Fig. 6A, C–D) and measure19.0–34.6 (X = 30.3) mm high × 20.3–40.9 (X = 31.6) mm wide, with a L/W ratio ranging from 0.8–1.1 : 1 (X = 0.97 : 1). Peduncles are 36.7–55.9 (X = 42.8) mm long by 0.9–1.1 (X = 0.95) mm wide. Each infructescence is made up of ~37 individual bilocular fruits that appear to be helically arranged on a central axis.

Styles are 4.1–6.3 (X = 5.2) mm long. In inflorescences, the styles are fleshy and extend into short, hooked tips (Fig. 6B, E). Mature infructescences have styles that have become brittle with elongately striate triangular bases that expand to ~4.9 mm wide (Fig. 6J). Within the areas between adjacent fruits are numerous knob-like extrafloral structures that have a ''braided'' appearance (Fig. 6C, D).

Fruits are 12.4 mm long × 4.3 mm wide (L/W ratio, 2.9 : 1), cylindrical to spindle-shaped, fused for ~2/3–3/4 of their total length, and free distally (Fig. 6H–I). Fruits are held together tightly (Fig. 6H), with relatively thin fruit walls. The fruit wall is composed of a uniseriate inner palisade layer and an outer pericarp (Fig. 6M). The palisade layer comprises individual cells that are radially elongate with a prominent thickened cell wall (Fig. 6G) and range in size from 12–15 μm long × 5–7 μm wide. Surface features of the inner carpel wall show short, rectangular cells, with oblique end walls (Fig. 7E, F). Cells are slightly raised above the general surface (Fig. 7J).

Seeds are 8.0 mm long × 2.3 mm wide (L/W ratio, 3.4 : 1), elongate, and have a relatively long distal wing (Figs. 7F, 8D). Cells of the seed coat are tangentially elongate, rectangular to polygonal with thickened anticlinal walls and mostly straight end walls (Fig. 8H). The epidermal cells of the seed coat are cuboidal in cross-section and are covered by a thin cuticle (Fig. 9H). Below the epidermis are 2–3 rows of small parenchyma cells followed by 2–3 rows of macrosclereids, each with a small lumen (Fig. 9H). To the inside of this fibrous layer are 2–3 rows of crushed epidermal cells of the outer integument, followed by parenchymatous cells of the endosperm (Fig. 9H).

Characteristic features of this species include the braided appearance of extrafloral processes, the broad style bases (Fig. 6C), the elongate seeds with a prominent distal wing, and the thickened cell walls of the inner carpel wall.

Phylogenetic analysis—Morphological cladistic analysis of *Liquidambar* and its close extant and fossil relatives with *Exbucklandia* and *Hamamelis* as outgroups revealed two MPT of 57 steps with a consistency index (CI) of 0.89, a retention index (RI) of 0.86, and a rescaled consistency index (RC) of 0.79 (Fig. 10A). The two trees differed in the position of the fossil *Liquidambar changii*. It was either sister to the extant *Liquidambar* clade (Fig. 10A) or formed a trichotomy with *L. acalycina* and the subclade of *L. formosana*, *L. orientalis*, and *L. styraciflua* (not shown). Of 42 character-state changes detected, 32 were parsimony informative. The family Altingiaceae is supported as monophyletic with the Cretaceous fossil from eastern North America, *Microaltingia apocarpela*, appearing as sister to the rest of the family. *Altingia* is sister to *Liquidambar*, which was also supported to be monophyletic by the morphological data. Within *Liquidambar*, the Miocene fossil taxon from western North America, *L. changii*, is cladistically basal. *Liquidambar acalycina* forms a clade with *L. formosana* and the subclade of *L. orientalis* and *L. styraciflua*.

Analysis of the *matK* data revealed one MPT of 115 steps with a CI = 0.99 and a RI = 0.98 (Fig. 10B). Of 114 character-state changes detected, 58 were parsimony informative. Altingiaceae were highly supported as monophyletic. *Liquidambar* was found to be paraphyletic with *Altingia chinensis* nested within it. *Liquidambar acalycina* and *L. formosana* are sisters, as are *L. orientalis* and *L. styraciflua*. *Altingia chinensis* was the sister to the clade of *L. acalycina* and *L. formosana*.

Both the partition-homogeneity test and the Templeton's significantly less parsimonious test (SLP_T) indicated that the morphological and the molecular *matK* data sets were not congruent (P = 0.01 and P = 0.0023, respectively). The conflicts between the trees of the two datasets (Fig. 10A, B) lay in the positions of *Altingia chinensis*, *L. acalycina*, and *L. formosana*. The morphological cladistic analysis supports the monophyly of *Liquidambar*. However, the molecular analysis suggests that *Altingia* was derived from within *Liquidambar* (Fig. 10B); specifically, it is sister to the *L. acalycina–L. formosana* clade.

The tree from the analysis constraining the monophyly of *Liquidambar acalycina* and *L. formosana* was four steps longer as compared to the unconstrained tree, with a CI = 0.83 and a RI = 0.75. When the morphological data was constrained against the *matK* phylogeny, excluding the two fossil taxa *Microaltingia apocarpela* and *L. changii*, the tree was nine steps longer, with a CI = 0.77 and a RI = 0.63. Constraining the three eastern Asian species (*Altingia chinensis*, *L. acalycina*, and *L. formosana*) as a clade, the tree was six steps longer with a CI = 0.81 and RI = 0.70.

←

resin canal, and tangentially elongate parenchyma cells next to the palisade-like inner carpel wall. **G.** Cross-section of pericarp with palisade-like inner carpel wall and tangentially elongate parenchyma cells, followed by an area of larger parenchyma cells. Note the start of breakage of this tissue at arrow. To the inside of this area are several vascular strands. **H.** Light micrograph of transverse section of stele from the central part of the infructescence in Fig. 6K. Pith is surrounded by prominent resin canals that are associated with primary xylem and a small amount of secondary xylem. **I.** SEM of vascular bundle with prominent fiber bundle sheaths surrounding vascular tissue. Scale bars: A–B = 1 cm, E = 1 mm, F, G = 300 μm, H–I = 50 μm. *Figure abbreviations*: br = breakage, bs = bundle sheaths, ep = epidermis, ic = inner carpel wall, rc = resin canal, sc = sclerenchyma, tpa = tangentially elongate parenchyma cells, vb = vascular strands, xy = vascular tissue.

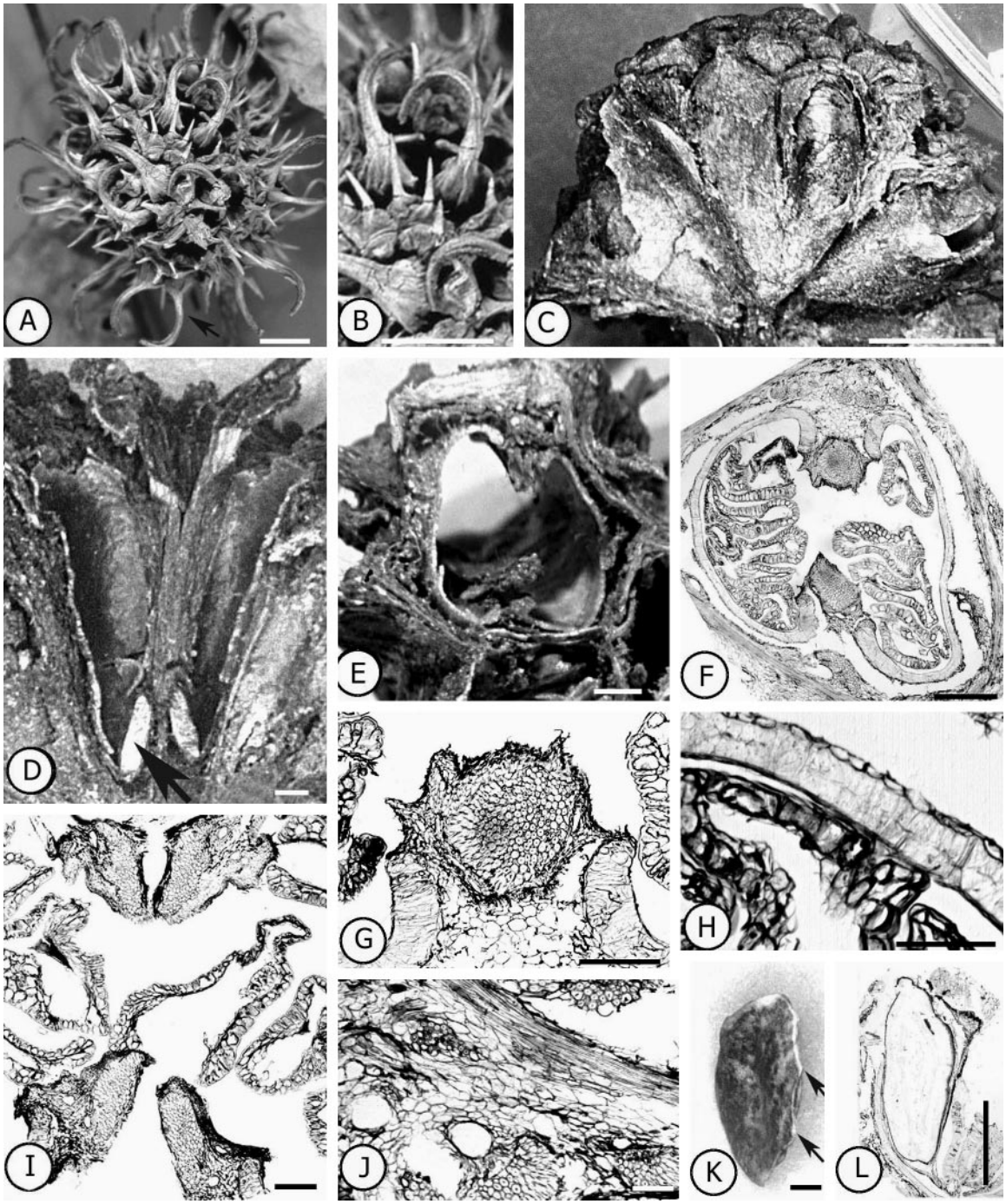

Fig. 3A–L. General features of *Liquidambar acalycina* infructescences. **A.** Overview of infructescence, showing paired, curved styles and prominent spines. Note that the paired styles of each bilocular fruit curve toward one another (arrow). **B.** Detail of paired styles. Note striate bases. Smaller spines attached to small protuberances have striate bases and are typically six per fruit. **C.** Longitudinal section of infructescence cut by hand-sectioning to reveal outer fruit morphology. Note that each bilocular fruit is separate and not tightly connected to adjacent fruits. **D.** Longitudinal section cut by hand-sectioning to reveal interior of locules. Carpels are fused toward base and free distally. Note prominent basal pads of tissue (arrow). **E.** Transverse section of fruit. Note separation of inner carpel layer from outer fruit wall. **F.** Transverse section of Paraplast-embedded fruit at proximal level where carpels are fused. Note expanded areas of fusion on ventral margins and tightly packed, aborted seeds. **G.** Detail of ventral margin showing pad of sclereids. **H.** Detail of 2-cell-layered, palisade inner carpel wall with layer of small, outer cells adhering. I. Transverse section of fruit at level distal to carpel fusion with detail of ventral margins separated along pads of sclereids. **J.** Detail of outer fruit wall showing vascular tissue and two prominent resin canals (lower left). **K.** External view of seed. Arrows indicate lateral flange (top), and hilum (bottom). **L.** Longitudinal section of seed showing lateral flange. Scale bars: A, L = 1 cm; B–C = 5 mm; D–F; K = 1 mm; I, G = 200 μm; H, J = 100 μm.

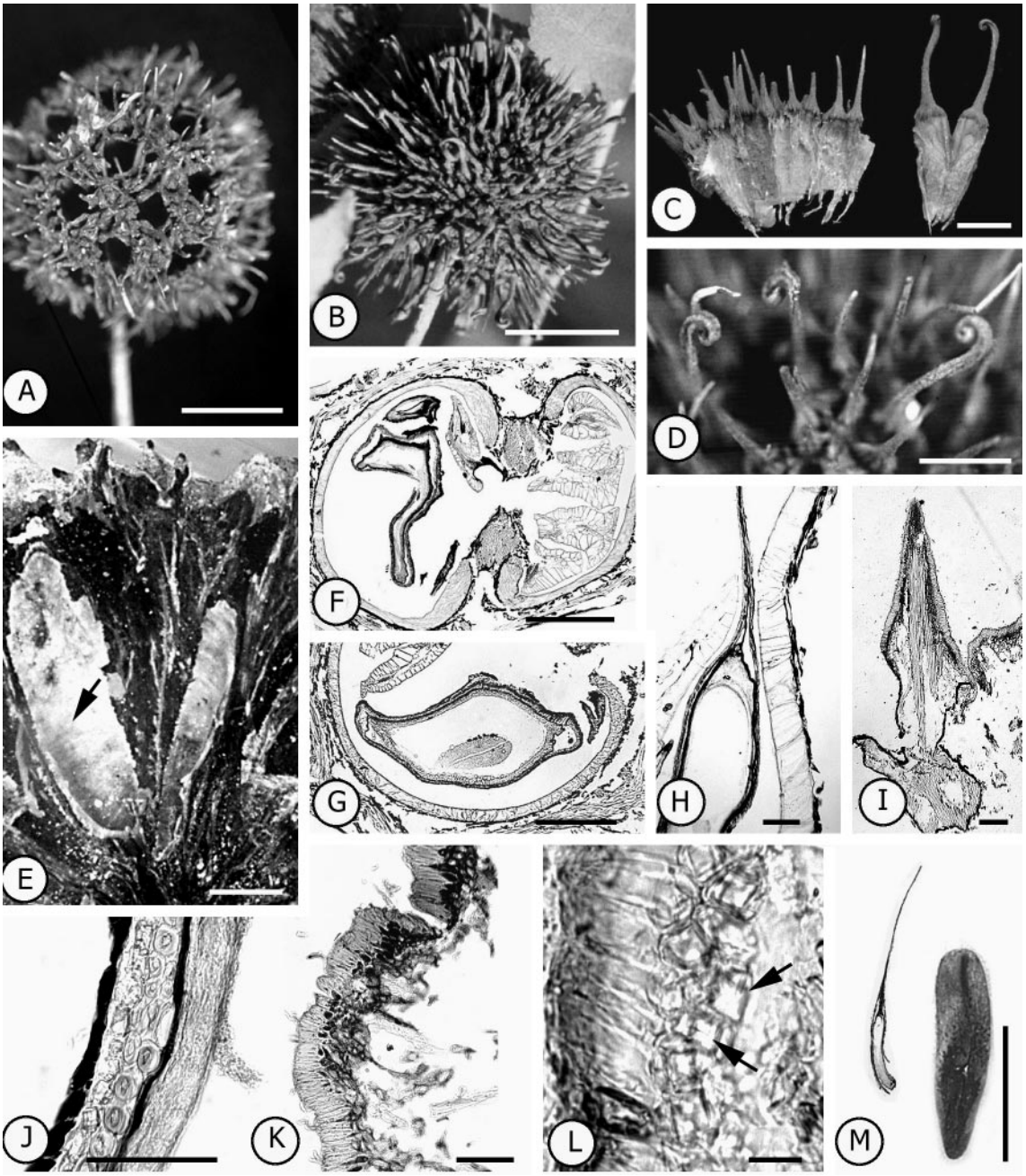

Fig. 4A–L. General features of *Liquidambar formosana* infructescences. **A., B.** Overview of infructescence. **C.** Hand-sections of individual bilocular fruit at right and series of extrafloral structures at left. **D.** Detail of coiled styles and straight extrafloral structures. **E.** Longitudinal hand-section to show inner carpel wall (arrow). **F.** Transverse section of Paraplast-embedded fruit at proximal level where carpels are fused. Note mature seed (left) and tightly packed aborted seeds (right). **G.** Transverse section of seed showing straight embryo with two cotyledons. **H.** Transverse section of single-layered inner carpel wall (right) and longitudinal section of seed showing distal wing (left). **I.** Longitudinal section of extrafloral structure with vascular tissue. **J.** Longitudinal section of seed coat showing outer epidermis (right) with a hypodermis containing druse crystals and a multilayered sclerenchyma layer next to a dark line of crushed inner integumentary walls. **K.** Transverse section of outer fruit wall appearing three-zoned, with outer palisade-like epidermis (left), and parenchymatous second zone (at right) grading into inner zone. **L.** Transverse section of seed coat showing prominent druses (arrows). **M.** Seeds with prominent distal wings, in longitudinal section (at left) and exterior view (at right). Scale bars: A, B = 1 cm; C, D = 5 mm; E = 2 mm; F, M = 1 mm; G, H, J, K = 100 μm; I = 300 μm L = 20 μm.

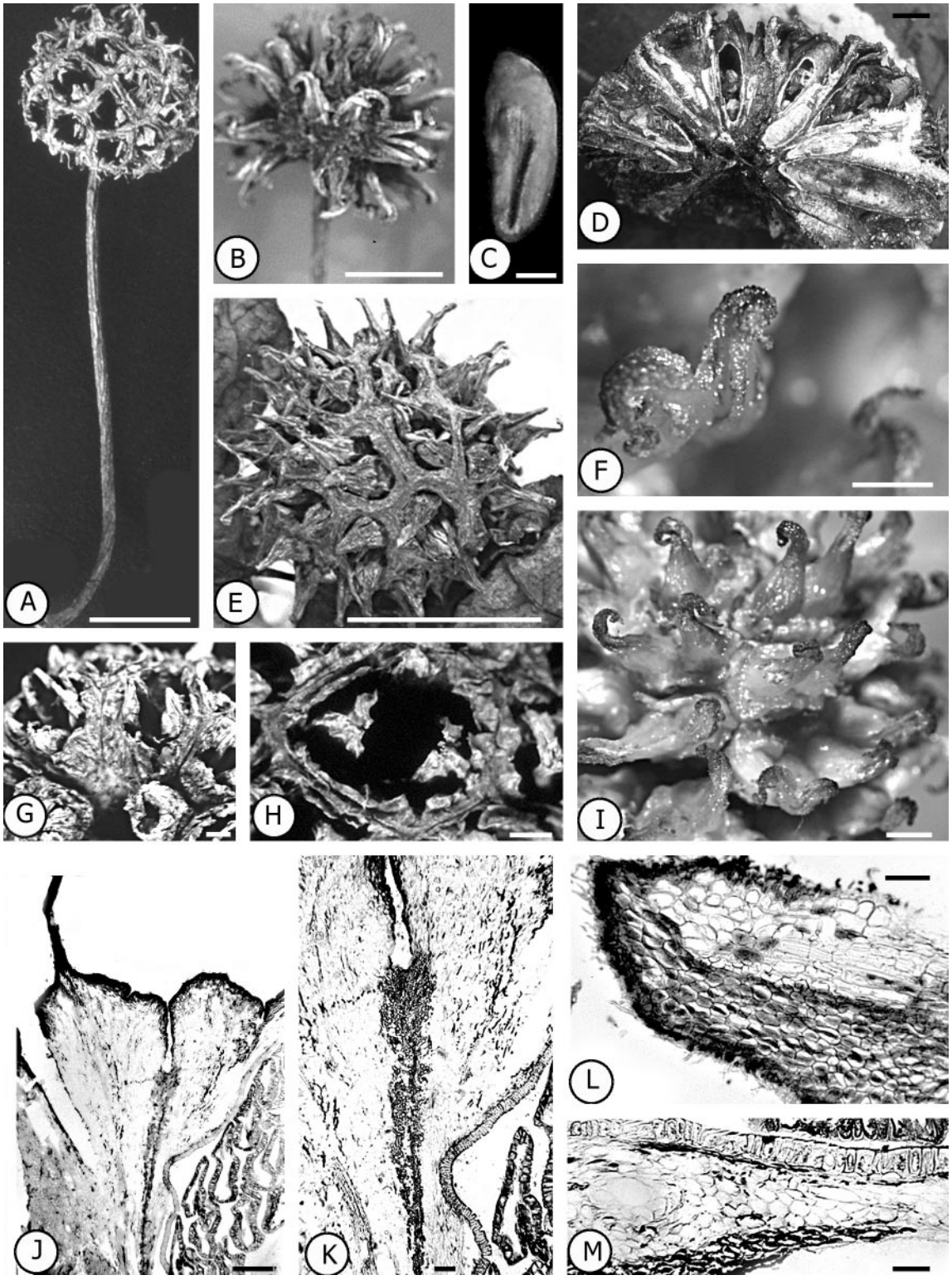

Fig. 5A–J. General features of *Liquidambar orientalis* infructescences and inflorescences. **A.** Overview of weathered infructescence. Note long peduncle. **B.** Overview of inflorescence with curved styles. **C.** Seed with distal wing. **D.** Longitudinal section through infructescence showing elongate, wedge-shaped locules. **E.** Overview of infructescence to show broad, smooth tissues between adjacent fruits (''peripheral rim''). **F.** Detail of stigmatic surfaces of adjacent styles. **G.** Detail of adjacent fruits showing thick tissue in center, and line of fusion (arrow) and styles. **H.** Detail of weathered fruit showing remnants of style bases. **I.** Inflorescence detail. Note curved styles with stigmatic surfaces covering outer layer. **J.** Longitudinal section of Paraplast-embedded fruit with wedge-shaped carpel and remnant of style (at top). **K.** Detail of fibers between adjacent fruits. **L.** Detail of lobed area between adjacent fruits. **M.** Detail of carpel wall showing inner single-celled palisade layer fused to outer fruit wall with resin canal (at left) and fibers. Scale bars: A = 1 cm; B = 5 mm; C, F, G, H = 1 mm; D, I = 2 mm; J, L, M = 50 μm; K = 200 μm.

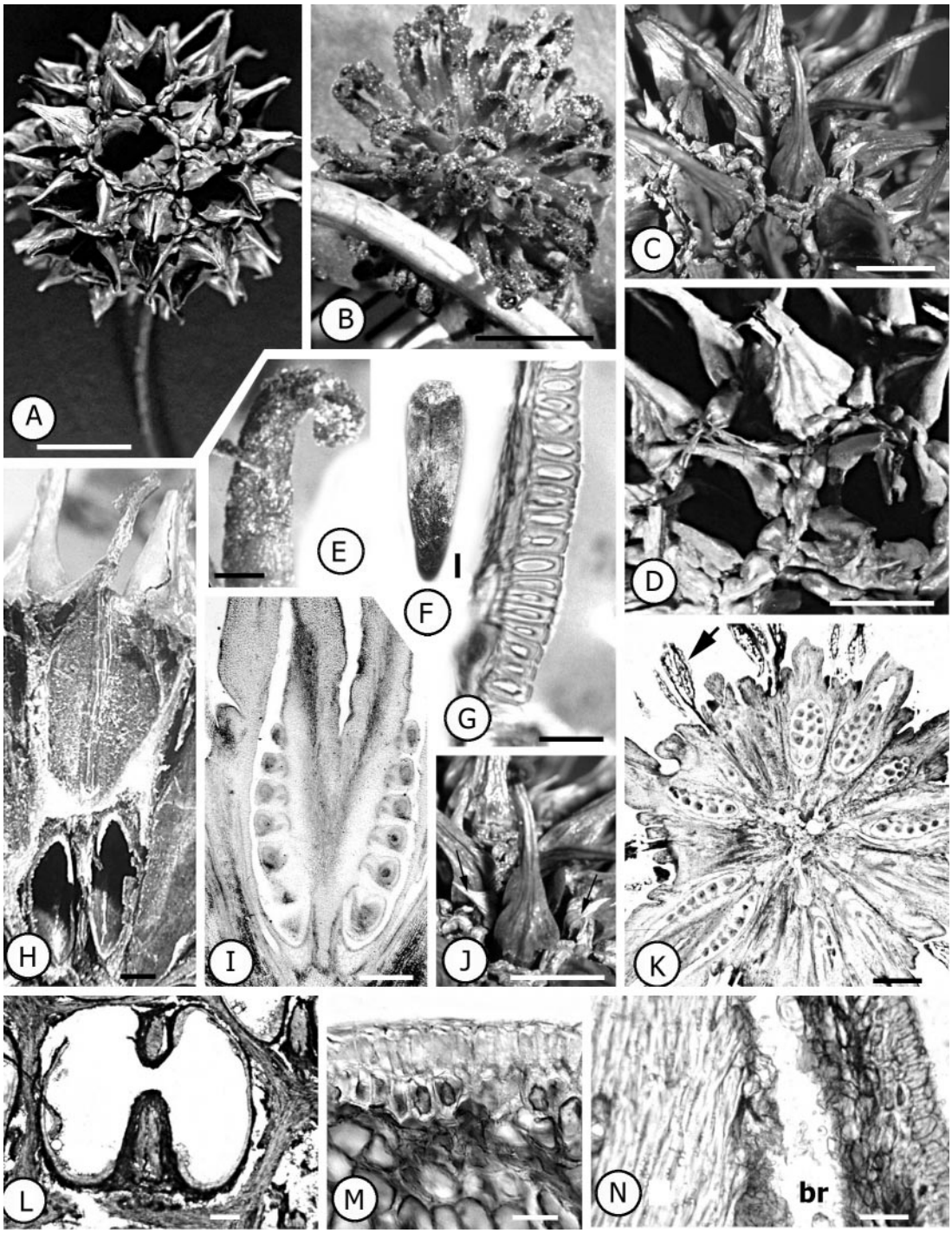

Fig. 6A–N. General features of *Liquidambar styraciflua* infructescences and inflorescences. **A.** Overview of infructescence. **B.** Overview of inflorescence. **C.** Detail of mature infructescence showing persistent style bases and ''braided'' intercapillary regions. **D.** Detail of mature infructescence showing persistent style bases, ''braided'' intercapillary ornamentation, and dehisced fruits. **E.** Detail of style from inflorescence with stigmatic surface. **F.** Seed with long distal wing. **G.** Detail of inner carpel wall. Note single cell layer with thickened cell walls. **H.** Longitudinal hand-section to show inner shape of bilocular fruit. **I.** Longitudinal section of gynoecium showing young developing anatropous ovules attached along margin. **J.** Detail of spinose extrafloral processes (arrows) among the otherwise ''braided'' ornamentation of tissue between adjacent fruits. **K.** Transverse section of inflorescence. Note stamen (arrow). **L.** Detail of sclerenchymatous ''pads'' from area of ventral fusion of carpels. **M.** Transverse section of pericarp showing tabular epidermal cells (top), and thick-walled hypodermal cells (below), followed by a parenchymatous layer (bottom). **N.** Transverse section of pericarp showing inner carpel wall (left) followed by tangentially elongate parenchyma cells and area where mature fruits tear. Scale bars: A, B = 1 cm; C, D = 5 mm; E, F, H = 1 mm; G, L, N = 100 μm; I = 500 μm; M = 50 μm. *Figure abbreviation:* br = breakage.

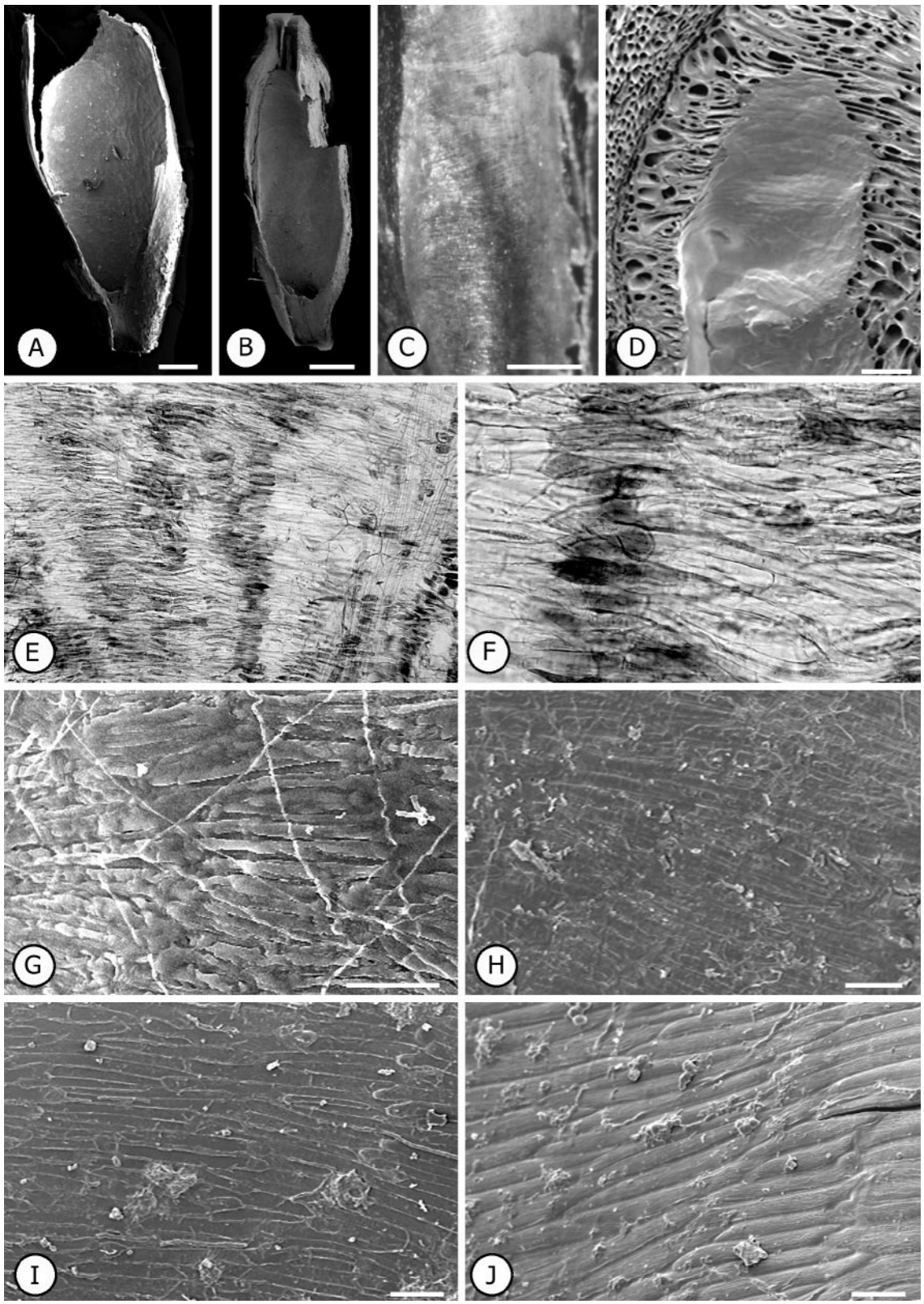

Fig. 7A–J. Detail of carpels in *Liquidambar*. **A.** Broadly obovate carpel of *L. acalycina*. **B.** Narrowly elongate carpel of *L. formosana*. C–D. *L. styraciflua*. **C.** Inner carpel wall appears as a distinct, lustrous layer in *L. orientalis*. **D.** Overview of inner carpel wall with thickened palisade cells at left of *L. styraciflua* **E.** Overview of inner carpel wall in transmitted light of *L. styraciflua*, note vascular strands at right. **F.** Details of individual carpel wall cells with oblique end walls of *L. styraciflua*. **G.** *L. acalycina* showing tangentially elongate cells that appear rod-like. **H.** *L. formosana* rectangular cells of the inner carpel wall with oblique end walls. **I.** *L. orientalis* showing rectangular inner carpel wall cells with oblique end walls. **J.** *L. styraciflua* inner carpel wall with rectangular cells that have oblique end walls. Scale bars: A–C = 1 mm, D = 100 μm, G–J = 50 μm.

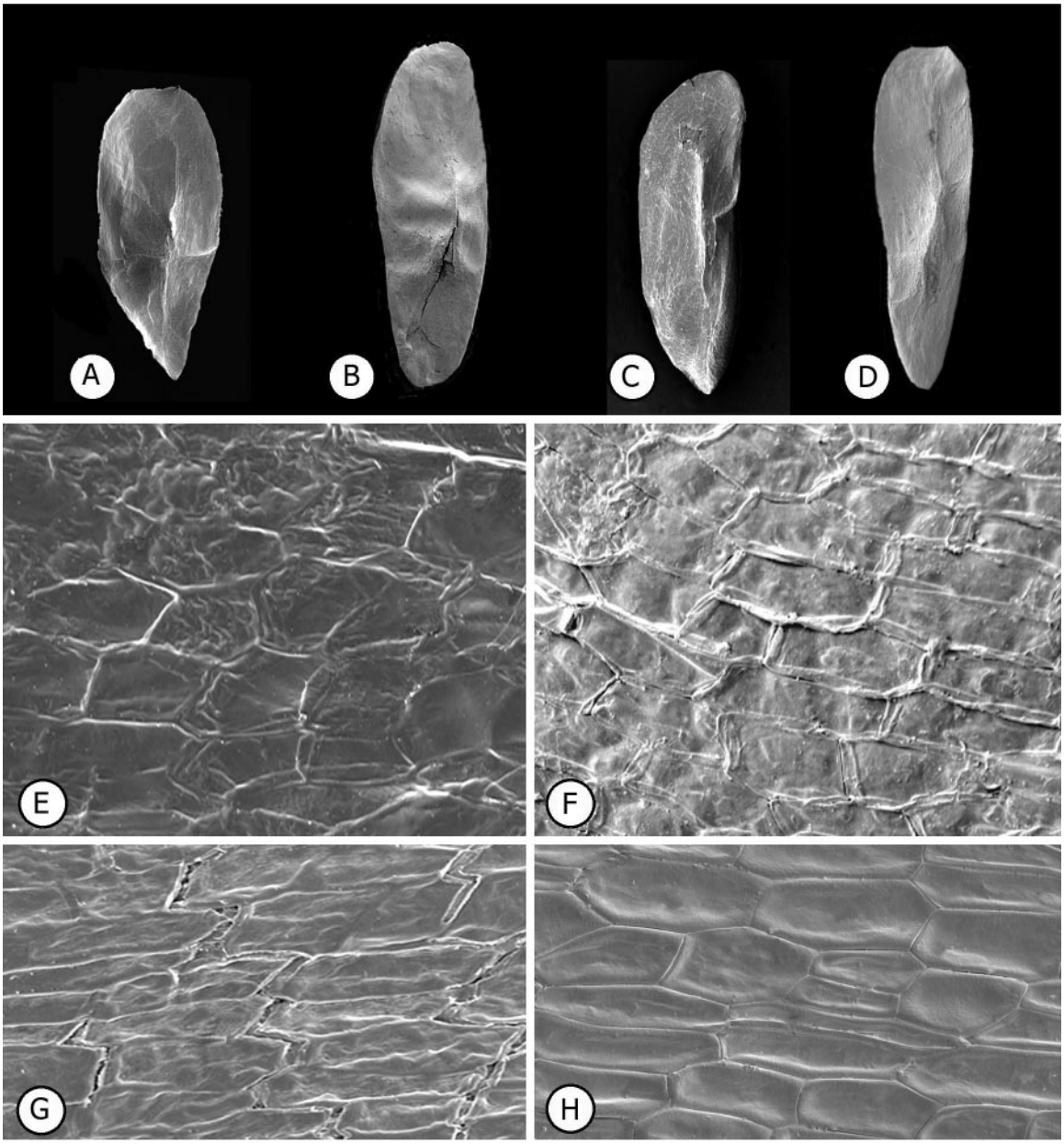

Fig. 8A–H. SEM micrographs of seeds and seed coat micromorphology in *Liquidambar*. A–D, Mature seeds; E–H, details of seed coat. **A.** *L. acalycina* seed with encircling flange. **B.** *L. formosana* seed with distal wing. **C.** *Liquidambar orientalis* seed with distal wing. **D.** *L. styraciflua* seed with distal wing. **E.** *L. acalycina*. **F.** *L. formosana*. **G.** *L. orientalis*. **H.** *L. styraciflua*. Scale bars: A–D = 1 cm, E–H = 50 μm.

DISCUSSION

Based on the comparative study of infructescence anatomy and morphology in *Liquidambar*, we can now identify several characters that appear to be both consistently reliable and taxonomically informative. They include some of the traditionally recognized characters, defined in more detail, as well as several new characters of anatomy and micromorphology. Among those we will discuss are (1) overall construction of infructescence; (2) infructescence size, shape, fruit number, and details of axis; (3) presence and type of extrafloral processes; (4) style morphology; (5) pericarp anatomy; (6) carpel surface micromorphology; (7) seed morphology; (8) seed anatomy; and (9) seed surface micromorphology.

Overall construction and structural integrity of infructescence—Infructescences vary in the degree to which fruits are attached to one another. In *L. styraciflua*, *L. orientalis*, and *L. formosana*, fruits are tightly attached: in *L. acalycina*, as in *Altingia*, fruits are loosely attached and the infructescence falls apart upon sectioning (K. Pigg, S. Ickert-Bond, personal observation). A similar organization occurs in the altingioid fossil infructescence *Steinhauera* Presl, which occurs in many European localities in the Eocene (Mai, 1968).

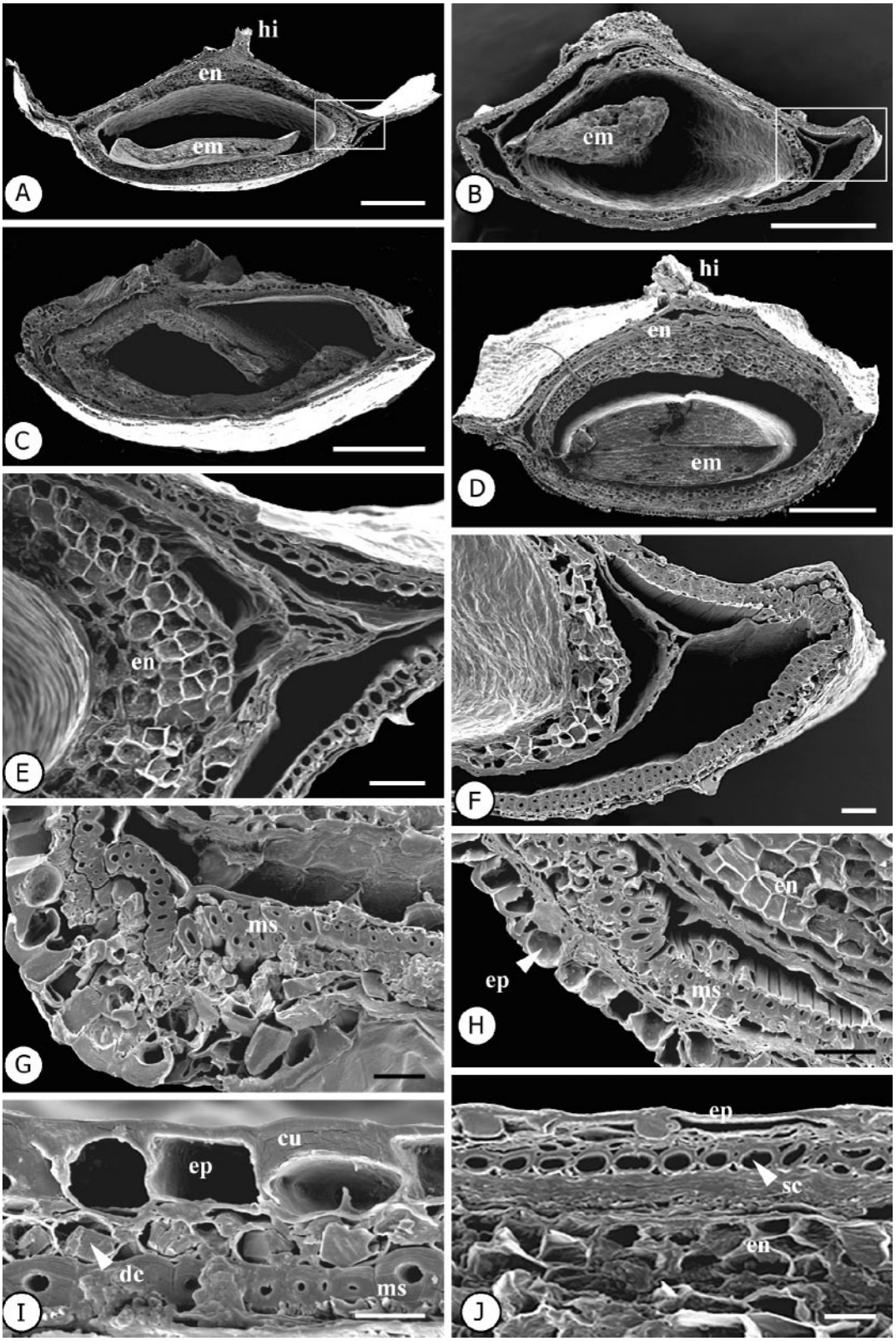

Fig. 9A–J. SEM micrographs of seed anatomy in *Liquidambar*. **A.** Transverse section of *L. acalycina* seed showing lateral flanges of the encircling wing. Note hilum at the top and the straight embryo in the center of the seed cavity, for details of boxed area see E. **B.** Transverse section of *L. formosana* seed with slightly enlarged flange of wing at the base on the right and embryo at center. For details of boxed area, see F. **C.** *L. orientalis* cross-section of seed lacking lateral flanges of the wing. **D.** *L. styraciflua* cross-section of seed with wing encircling the seed but not as expanded as in A. **E.** *L. acalycina* details of single layer of sclerenchyma with large lumen. Note parenchymatous cells of the endosperm. **F.** *L. formosana* details of multiple layers of macrosclereids with small lumen and inner integument. **G.** *L. orientalis* showing several layers of macrosclereids. **H.** *L. styraciflua* showing thin cuticle above cuboidal epidermal cells.

Infructescence size, shape, fruit number and details of axis—The number of fruits per infructescence varies with *L. orientalis* having the largest number (48), *L. styraciflua* and *L. formosana* with fewer (37 and 34, respectively), and *L. acalycina* with the fewest (26). The relative size of infructescences also varies, with the largest infructescences found in *L. styraciflua* (30 mm long), those of intermediate size in both *L. acalycina* and *L. formosana* (27 mm long), and those of *L. orientalis*, the smallest, at only 15 mm. Width varies accordingly within individual measurements (Table 2), and comparable relative dimensions are found in carpel size. In our observation it is interesting to note that *L. orientalis* has a much smaller infructescence with considerably more fruits than the other species of *Liquidambar*. When scaled to the same infructescence size, *L. orientalis* has twice as many fruits as *L. formosana*, three times as many fruits as *L. acalycina*, and 2.4 as many fruits as *L. styraciflua*. Although all four species have spherical infructescences, *L. orientalis* is somewhat wider than long, with a L/W ratio of 0.9 : 1. In comparison to these extant species, the Cretaceous fossil, *Microaltingia*, is tiny (~7 mm in diameter) with 8–12 fruits, and the Miocene *L. changii* around 2.5 cm in diameter with approximately 25–30 fruits per head (Zhou et al., 2001; Pigg et al., 2004).

Presence and type of extrafloral processes—The presence or absence of extrafloral processes has been historically important in the delimitation of species of *Liquidambar* (Harms, 1930). In our study we observed that all species of *Liquidambar*, as well as several representative species of *Altingia*, typically have a group of 8–12 extrafloral structures of some sort surrounding each mature fruit. The presence of these types of structures throughout Altingiaceae was noted previously (Bogle, 1986). The most obvious of these are the ''extra spines'' of *L. formosana* (Fig. 4C); however, spinose structures also occur in *L. acalycina* (Fig. 3B). Braided knob-like structures as well as occasional short spinose protuberances occur in *L. styraciflua* (Fig. 6A, C), and broad, slightly raised ''smooth'' areas occur in *L. orientalis* (Fig. 5A). In *Altingia*, structures found in the same positions are mostly small tubercles (S. Ickert-Bond, unpublished data).

These extrafloral processes have variously been described by the neutral term phyllome (sensu Esau, 1965) by Bogle (1986) or interpreted as (1) bracteoles (Guillaumin, 1920), (2) staminodia (Tong, 1930), (3) calyx lobes (Chang, 1962, 1973), (4) papillae on the surfaces of the capsules (Schmitt, 1965), or (5) as vestigial styles of sterile flowers interspersed among fertile flowers (Harms, 1930). In their ontogenetic study, Wisniewski and Bogle (1982) observed that the extrafloral processes developed late in *L. styraciflua*, well after stamens and functional carpels were initiated. However, their observations do not resolve the homology of these structures.

To determine the homologies of these extrafloral processes, we considered the morphology, position, and merosity of the five types of structures previously proposed as homologous by various authors. If, for example, the extrafloral structures are homologous with (1) bracteoles or modified leaves associated with the inflorescence (Gifford and Foster, 1989), one would expect only a single pair of these structures to occurr alternately at the base of each gynoecium, as in the closely related hamamelid clade, and that they would most likely appear leafy. If they are homologous with (2) staminodia, transitional forms leading to stamens would be expected (Bogle, 1986). Within the closely related Hamamelidaceae, rare reports of sterile phyllomes transitional to stamens are known from *Corylopsis* Siebold et Zucc. (Tong, 1930; Endress, 1967) and *Loropetalum* R. Br. (Mione and Bogle, 1990). If the structures are homologous to (3) calyx lobes, they would quite likely conform to the merosity of the floral parts within the closely related hamamelids. Among hamamelids that develop a perianth, the calyx is four to five-merous; however, in those lacking a well-developed corolla, the organ merosity is not fixed (Endress, 1989c). The structures are unlikely to be homologous with (4) papillae, as they are vascularized, woody, and composed of multiple layers of cells.

Of these several alternatives, the most probable explanation to us is that the extrafloral structures are homologous to (5), a group of nondeveloping flowers that surround a viable flower. Our interpretation is supported by the similar morphology of these structures, particularly those of *L. acalycina* and *L. formosana*, with viable fruits, and their often paired appearance, as would be expected if these structures are derived in the same way as the bilocular fruits of Altingiaceae.

To better understand whether this interpretation might be valid, we made small clay models of normal-sized and smaller bilocular fruits and positioned them together on a branching system (Fig. 2D). The resulting model has 8–10 small ''extrafloral processes'' surrounding a ''viable flower.'' The actual number of surrounding processes would be somewhat variable, because of the small amount of torque expected in the tightly packed, helically arranged fruits. Despite their superficial differences, the well-developed spinose extrafloral structures of *L. acalycina* and *L. formosana*, the ornamented ''braided'' peripheral rims of *L. styraciflua*, and the broad areas between fruits of *L. orientalis* are found in the same relative positions, supporting a positional criterion of homology (e.g., Kaplan, 1984).

Styles in inflorescences and infructescences—Persistent styles are typically characteristic of mature infructescences of *Liquidambar* (Bogle, 1986; Ferguson, 1989); however, information on the morphology of styles within inflorescences at anthesis is mostly lacking (Tardieu-Blot, 1965). This character was studied in greater detail. Styles within inflorescences are fleshy and thick in *L. styraciflua* and *L. orientalis*, and considerably narrower in *L. formosana*. The stigmatic surfaces in all species are relatively broad and decurrent (Bogle, 1986; Endress and Igersheim, 1999). In *L. styraciflua* and *L. orientalis*, the fleshy stigmas end in a short, curving tip upon which the stigmatic surface occurs. In contrast, the styles of *L. formosana* are distinctly coiled. Fresh inflorescences of *L. acalycina* were not available for study; however, from examination of inflorescences on herbarium sheets the styles in *L. aca-*

←

Note several layers of macrosclereids and parenchymatous endosperm. **I.** *L. orientalis* showing thick cuticle on epidermis. Note druse crystals in the hypodermis above thick-walled macrosclereids. **J.** *L. acalycina* showing rectangular shaped epidermal cells and sclereids with a large lumen (compare to I). Note parenchymatous cells of the endosperm. Scale bars: A–D = 1 mm, E–H = 50 μm, I–K = 20 μm. *Figure abbreviations*: cu = cuticle, dc = druse crystal, em = embryo, en = endosperm, ep = epidermis, hi = hilum, ms = macrosclereids, sc = sclereids.

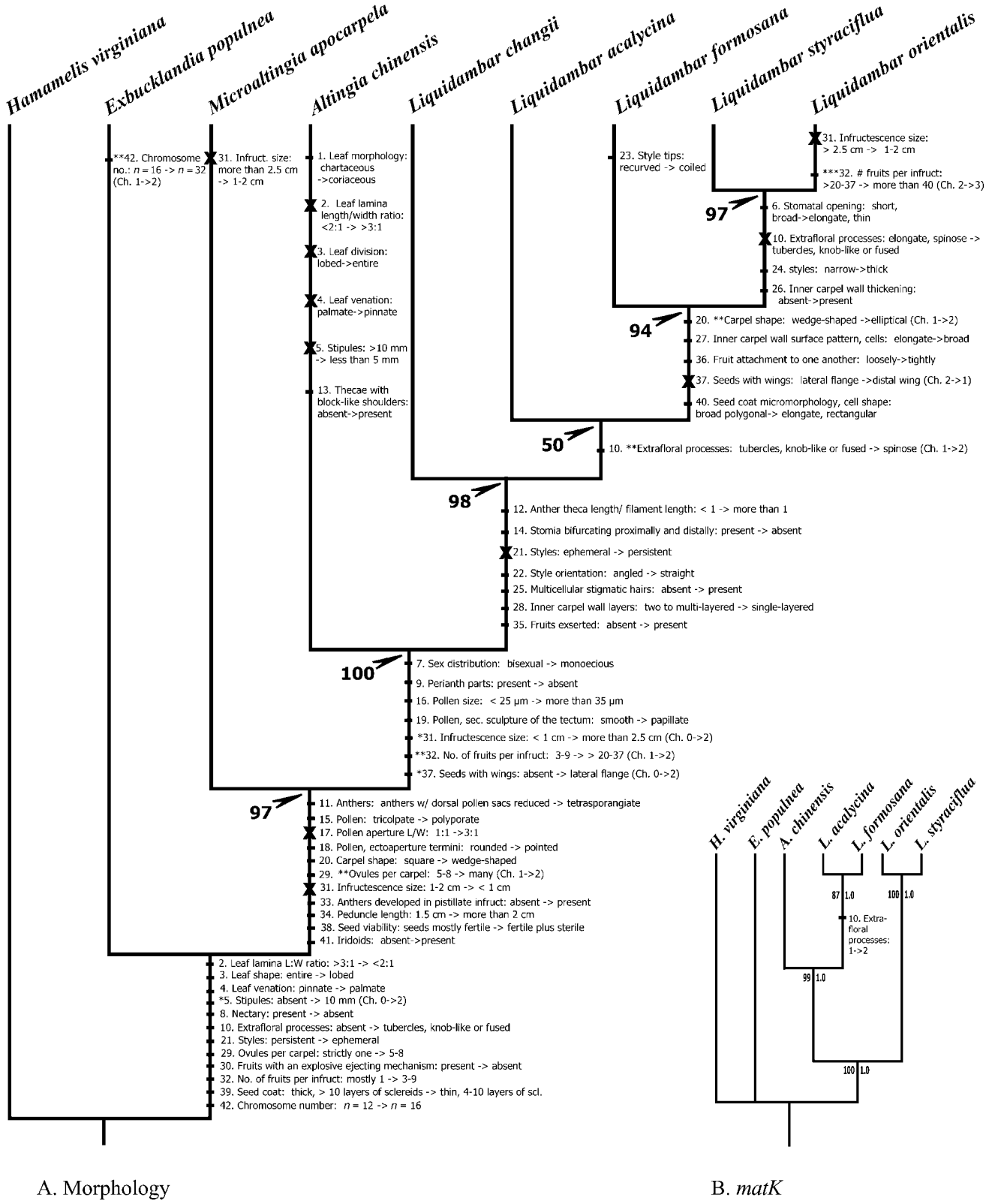

Fig. 10. Two hypotheses of relationships in Altingiaceae based on analysis of (A) morphology and (B) *matK* sequences. Trees shown are single most parsimonious trees. Numbers next to arrows reflect bootstrap support values in (A), while in (B), numbers to the right of the branches are bootstrap support and on the left are posterior probabilities equal or above 0.95 from a Bayesian MCMC tree sampling procedure. Most character state changes are changes from 0 to 1, other changes are specifically marked: * = changes from 0 to 2, ** = changes from 1 to 2, *** = changes from 2 to 3, and reversal are marked by an ''X'' on the phylogeny.

lycina appear narrow. The stigmatic surfaces of *Liquidambar* are unusual in having unicellular papillate epidermal cells superimposed on multicellular protuberances, while the stigmatic surfaces of the Hamamelidaceae are generally described as mostly not papillate, but with pluricellular warts (Endress, 1989b, 1993; Endress and Igersheim, 1999). As the infructescences develop, styles of all species tend to dry out and become woody and brittle. The stigmatic surfaces often break off or abrade at this stage; however, the styles and their triangular bases typically persist (Figs. 3A, 3B, 4A, 5E, 6A, 6C). With desiccation the styles and style bases become vertically striate (Figs. 3B, 4C, 6C).

Carpel/locule shape—All fruits of *Liquidambar* are spherical infructescences with numerous bilocular fruits packed into a sphere. There is variation in the shape of carpels. *Liquidambar formosana* and *L. styraciflua* have elongate locules (Figs. 4C, 4E, 6H, 6I), those of *L. orientalis* are obovate (Fig. 5D), and those of *L. acalycina* are broadly obovate (Fig. 3C). Those of *Microaltingia* and *L. changii* can be compared most favorably with those of *L. acalycina* (Zhou et al., 2001; Pigg et al., 2004).

Pericarp anatomy—We demonstrate for the first time that characters of pericarp anatomy vary among different species of *Liquidambar*. In particular, the innermost layer of palisade cells that lines each locule varies in cell number and anatomy. It is a single cell thick in *L. styraciflua* (Fig. 6E), *L. orientalis* (Fig. 5M), and *L. formosana* (Fig. 4H) and two cells thick in *L. acalycina* (Fig. 3H). Among species with a single palisade, *L. formosana* has cells with thin walls (Fig. 4H), while in *L. styraciflua* (Fig. 6E) and *L. orientalis* (Fig. 5M), cells have a prominent thickening on the inner tangential wall. In contrast, organization of the inner part of the outer pericarp is similar in all species, with fragments of the innermost tangentially oriented cell layers typically adhering to the inner palisade layer. The ground tissues of mature infructescences are often difficult to characterize because they are usually ruptured and torn along planes of weakness, particularly within the area inside of the vascular strands (Fig. 2E). To the outside, the vascular bundles among species vary further with the presence or absence of druses, differences in number and distribution of resin canals, and amounts and type of sclerenchyma (Figs. 3F, 3J, 4F, 4K, 4L, 5K, 5L). The epidermis also varies among species, with *L. acalycina* and *L. styraciflua* (Fig. 4K) characterized by tabular cells, *L. orientalis* by papillate types (Fig. 5L), and *L. formosana* by radially elongate cells.

Carpel surface micromorphology—The innermost carpel wall appears as a distinct lustrous layer during hand-sectioning of infructescences in *Liquidambar* (Figs. 4E, 7C) and separates readily from the remaining pericarp. Surface micromorphology has a fairly homogenous cell pattern with short rectangular cells, that have oblique end walls in *L. formosana* (Fig. 7H), *L. orientalis* (Fig. 7I), and *L. styraciflua* (Fig. 7J). In contrast, *L. acalycina* has tangentially elongate cells that appear rodlike and anastomose (Fig. 7G).

Seed morphology—Whereas the large majority of genera in the closely related family Hamamelidaceae s.s. have ballistic seeds lacking a wing, those of the Altingiaceae have either distally winged or circularly flanged seeds (Tiffney, 1986; Fig. 2H). Wing morphology ranges from large distal wings in *L. styraciflua* (Fig. 6F) and *L. formosana* (Fig. 4M) to somewhat shorter wings in *L. orientalis* (Fig. 5C), while *L. acalycina* has small circular to triangular wings that are similar to those of both *Semiliquidambar* and *Altingia* (Fig. 3K, L; S. Ickert-Bond, unpublished data). Seeds of the fossil *L. changii* have circular flanges (Pigg et al., 2004), while those of *Microaltingia* are reported to lack wings (Zhou et al., 2001). Seeds in Altingiaceae are typically speckled or striped, but variation in this feature, even within a single infructescence, does not allow for species delineation based on this character.

Seed anatomy—Another feature that has been described previously for some taxa formerly recognized within Hamamelidaceae (including *Liquidambar*) is seed anatomy (Shoemaker, 1905; Melikian, 1971, 1973; Rao, 1974; Zhang and Wen, 1996). In *Liquidambar*, the outer epidermis of the inner integument constitutes most of the seed coat, in contrast to most hamamelidaceous seeds, in which the tegmen does not contribute much to the seed coat (Rao, 1974). The seed coat in *Liquidambar* is well differentiated. A uniseriate epidermis is covered by a cuticle on upper anticlinal walls in *L. formosana* (Figs. 4J, 8J), while in both *L. styraciflua* and *L. orientalis*, the cuticle is found on both anticlinal and periclinal walls (Fig. 8I; Melikian, 1973). A uniseriate hypodermis contains druse crystals in *L. styraciflua* (Fig. 8I, K), *L. formosana* (Fig. 4J), and *L. orientalis*, while we failed to find them in *L. acalycina*. To the inside of the hypodermis are 1–3 layers of macrosclereids. Both *L. orientalis* and *L. styraciflua* have macrosclereids in 1–2 rows, while in *L. formosana* there are 2–3 rows. In a detailed study of seed coats in Hamamelidaceae, Melikian (1973) concludes that the very thin seed coats of *Liquidambar* and *Altingia* are specialized in comparison to the relatively thick seed coats in the rest of the Hamamelidaceae s.s., which was considered ''primitive.''

Seed surface micromorphology—Overall seed surface micromorphology in *Liquidambar* is relatively homogeneous with cells arranged parallel to the long axis of the seed (Fig. 8E–H). The surface of seed coats in *L. acalycina* differs from the other three species in having polygonal (4–5 sided) cells that are slightly elongate and appear slightly thickened on the anticlinal walls (Fig. 8E), while the other taxa have tangentially elongated and rectangular cells with thickened anticlinal walls (Fig. 8F). Among the three species with rectangular cells of the seed coat, *L. styraciflua* (Fig. 8H) and *L. formosana* (Fig. 8F) have straight end walls, while *L. orientalis* has oblique end walls (Fig. 8G).

Evolution of fruit dispersal in Altingiaceae—Although the genera comprising the Altingiaceae have been recognized as closely related to those members of the Hamamelidaceae s.s., there are several important differences between these two groups that have, in part, led to the recognition of the Altingiaceae as a distinct family (Judd et al., 2002). The Altingiaceae are distinguished from the Hamamelidaceae s.s. by the presence of polyporate rather than tricolpate pollen. They also have multiseeded, bilocular carpels, that lack an elaborate dispersal mechanism, in contrast to the single-seeded capsules of the Hamamelidoideae of Hamamelidaceae, which have an explosive (ballistic) ejection mechanism (Tiffney, 1986; Endress, 1993). *Exbucklandia* (Exbucklandioideae) and *Rhodoleia* (Rhodoleioideae) also lack this explosive dispersal syndrome

(Endress, 1989b), suggesting that the ballistic dispersal is perhaps a synapomorphy for subfamily Hamamelidoideae.

Within *Liquidambar*, *L. formosana* and *L. styraciflua* have elongate locules (Figs. 4C, 4E, 6H, 6I), those of *L. orientalis* are obovate (Fig. 5D), and those of *L. acalycina* are broadly obovate (Fig. 3C). There is a correlation between seed shape and locule shape, with seeds with elongate distal wings in *L. formosana* and *L. styraciflua*, and those with a shorter distal wing in *L. orientalis*. *Liquidambar acalycina* seeds have a circular to triangular flange encircling the seed body, and its locules are considerably shorter and broader. Carpel surface micromorphology correlates with this as well, as does the overall construction and structural integrity of infructescences. It is interesting that while the first three species have tightly interconnected infructescences, those of *L. acalycina* are only loosely attached to one another. The fossil *L. changii* has locules and seeds with shapes similar to those of *L. acalycina* (Pigg et al., 2004).

In comparison to the hamamelids with a ballistic or explosive dispersal mechanism, the composition and structure of infructescences of the Altingiaceae with 1-several seeded fruits, crowded and partially immersed in an infructescence, functionally constrains these taxa to a nonballistic dispersal mechanism (Endress, 1989c). Within the family, several variations of dispersal have evolved. Whereas in general, the more elongate seeds of *Liquidambar* are abiotically dispersed, Vink (1957) reports monkeys, birds, and ants feeding on the shorter, fatter seeds of the closely related *Altingia excelsa* Nor., which Kalshoven (1937) describes as containing oil.

Differences in seed and locule shape among species of *Liquidambar* seem also to play a role in dispersal, because the broader seeds of *L. acalycina* and the fossil *L. changii* would have to have a broader opening during dehiscence as compared to the slender, elongated seeds of the other three extant species of *Liquidambar*. Many wind-blown infructescences contain the large viable seeds inside, while only the smaller aborted seeds have been displaced from within the pendulous infructescences.

Morphological evolution of Liquidambar—The morphological cladistic analysis supports the monophyly of *Liquidambar*. However, the molecular analysis suggests that *Altingia* is nested within *Liquidambar* (Fig. 10B); specifically, it is sister to the *L. acalycina–L. formosana* clade. Morphological characters that differentiate *Liquidambar* from *Altingia* include size and shape of inflorescence, number of florets (and fruits) per head, presence or absence of spines in the infructescence, persistence of styles on infructescence, and mode of fruit dehiscence (Ferguson, 1989; Zhang et al., 2003). *Semiliquidambar* has morphology intermediate between the two other genera and is thought by some to be an intergeneric hybrid (Bogle, 1986; Ferguson, 1989). A rigorous study examining infructescence diversity in *Altingia* and *Semiliquidambar* based on material recently collected is currently underway.

Our morphological cladistic analysis suggests the following seven synapomorphies for *Liquidambar*: (1) filaments longer than anthers, (2) absence of stomium bifurcations, (3) persistent and (4) straight styles, (5) presence of multicellular stigmatic hairs, (6) single-layered inner carpel walls, (7) exserted fruits (Fig. 10A). *Liquidambar formosana* shares several morphological characters with *L. orientalis* and *L. styraciflua*: elliptical carpel shape, broad cells of the inner carpel wall, seed with a distal wing, and rectangular epidermal cells of the seed coat surface. However, the phylogenetic analysis of the *mat*K gene supports the monophyly of *L. formosana* and *L. acalycina* (Fig. 10B). When constraining the monophyly of *L. formosana–L. acalycina* in the morphological data, the tree would have four additional steps as compared to the unconstrained analysis. The *L. formosana–L. acalycina* clade is only weakly supported morphologically with one synapomorphy (spinose extrafloral structures) as revealed in the apomorphy list in PAUP* (Fig. 10B).

Different positions of *Altingia chinensis* are revealed in the morphological analysis as compared to the molecular data set. In the morphological analysis, *Altingia chinensis* is sister to the *Liquidambar* clade (Fig. 10A), whereas in the molecular tree it is sister to the *L. acalycina–L. formosana* clade (Fig. 10B). When we constrain the morphological data with the *matK* topology, the tree would have nine additional steps as compared to the unconstrained analysis, but there were no detectable morphological synapomorphies for the relationship of (*A. chinensis* (*L. acalycina*, *L. formosana*)) in our data set. Constraining the monophyly of the unresolved *A. chinensis–L. acalycina–L. formosana* clade revealed a tree six steps longer than the unconstrained tree. This eastern Asian clade within *Liquidambar* (*L. acalycina* and *L. formosana*) is supported by one synapomorphy, the presence of spinose extrafloral processes.

The discordance between the morphological and the molecular data concerning the position of *Altingia* may be due to different rates of morphological evolution and convergence. *Altingia* differs significantly from *Liquidambar* morphologically. At least seven differences are autapomorphic for *Altingia*, whereas few or no autapomorphies were detected for each of the four species of *Liquidambar* (Fig. 10A). Among the seven are three reversals suggesting convergence may also have played a role in the morphological patterns we detected. *Altingia* and *Liquidambar acalycina* share the following morphological characters: wedge-shaped carpels, the inner carpel wall lined with elongate cells, loose attachment of fruits to one another, seeds with a circular flange, and polygonal cells of the seed coat surface. In the morphological analysis, these shared characters are symplesiomorphies. We are currently documenting the morphology of additional taxa for *Altingia* to better evaluate patterns of morphological diversification in Altingiaceae.

Taxonomic implications—Two sections have traditionally been recognized within *Liquidambar*: sect. *Liquidambar* and sect. *Cathayambar* (Harms, 1930). Harms (1930) used the presence of ''Borsten,'' or ''setae'' sensu Bogle (1986), here considered extrafloral spinose structures, in the inflorescences and infructescences of *L. formosana* as the defining character for his section *Cathayambar*. The remaining species (*L. orientalis* and *L. styraciflua*) were placed in sect. *Euliquidambar* (= *Liquidambar*) and were stated as lacking these structures. When *Liquidambar acalycina* was described (Chang, 1959), it was placed in sect. *Liquidambar* along with *L. orientalis* and *L. styraciflua*, partly on the basis of a lack of extrafloral spinose structures. However, neither the morphological phylogeny nor the *matK* tree supports the placement of *Liquidambar acalycina* in sect. *Liquidambar* (Fig. 10A, B). The molecular data so far clearly suggest the paraphyly of *Liquidambar* (Fig. 10B). The *matK* phylogeny also shows a strongly supported clade of the eastern Asian (*L. acalycina*, *L. formosana*) sister to *Altingia chinensis*. Previous studies stated that the presence

of the spinose extrafloral structures is autapomorphic for *L. formosana* (Li et al., 1997a), but we observed comparable structures in the inflorescences and infructescences of *L. acalycina* (Fig. 3A, B). This character is the only synapomorphy detected so far for the *L. acalycina–L. formosana* clade in analysis of morphology (Fig. 10B). With the completion of nomenclatural changes to be made for Altingiaceae (S. Ickert-Bond and J. Wen, unpublished data), the taxonomic significance of morphological characters will be further evaluated.

Biogeographic implications—The intercontinental disjunction of *Liquidambar* in the northern hemisphere has sparked much interest in recent years (Hoey and Parks, 1991, 1994; Shi et al., 1998; Li and Donoghue, 1998). All available data so far suggest a close relationship between the eastern North American *L. styraciflua* and the western Asian *L. orientalis*. Consideration of the fossil evidence of Altingiaceae revealed much more complex intercontinental biogeographic relationships (Zhou et al., 2001; Pigg et al., 2004). Our studies suggest that the Middle Miocene fossil from western North America, *Liquidambar changii*, is sister to a clade of extant *Liquidambar* (*L. acalycina*-eastern Asia (*L. formosana*-eastern Asia (*L. styraciflua*-eastern North America, *L. orientalis*-western Asia))). Furthermore, the Cretaceous fossil from eastern North America, *Microaltingia apocarpela*, is suggested to be sister to the clade consisting of the rest of Altingiaceae, which adds another intercontinental disjunction within Altingiaceae. We are currently constructing a phylogeny of the family with multiple molecular markers, morphology, and additional fossil data to better understand the evolution of intercontinental biogeographic disjunctions in the Northern Hemisphere.

LITERATURE CITED

ANGIOSPERM PHYLOGENY GROUP (APG II). 2003. An update of the Angiosperm Phylogeny Group classification for the orders and families of flowering plants: APG II. *Botanical Journal of the Linnean Society* 141: 399–436.

ARCHIE, J. W. 1985. Methods for coding variable morphological features for numerical taxonomic analysis. *Systematic Zoology* 34: 326–345.

BLUME, C. L. 1828. Flora Javae. J. Frank, Brussels, Belgium.

BOGLE, A. L. 1986. The floral morphology and vascular anatomy of the Hamamelidaceae: subfamily Liquidambaroideae. *Annals of the Missouri Botanical Garden* 73: 325–347.

BORATYNSKA, K. 1984. Distribution of *Liquidambar orientalis* Mill. on Rhodos Island. *Arboretum Kornickie* 29: 3–11.

CARLQUIST, S. 1982. The use of ethylene diamine in softening hard plant tissue for paraffin sectioning. *Stain Technology* 57: 311–317.

CHANG, K. T. 1959. The pollen morphology of *Liquidambar* L. and *Altingia* Nor. *Botaneski Zhurnal* 44: 1375–1380.

CHANG, H.-T. 1962. *Semiliquidambar*, novum Hamamelidacearum genus *Sinicum*. *Sunyatsen University Bulletin of Natural Science* 1: 34–44.

CHANG, H.-T. 1973. A revision of the Hamamelidaceous flora of China. *Bulletin of Sun-Yatsen University* 1: 54–71.

CHANG, H.-T. 1979. Hamamelidaceae. *In* H.-T. Chang [ed.], Flora Reipublicae Popularis Sinicae, vol. 35 (2), 36–116. Science Press, Beijing, China.

CHANG, T.-T. 1964. Pollen morphology of Hamamelidaceae and Altingiaceae. *Acta Insituti Botanici Nomine V. L. Komarovii Academiae Scientiarum Unionis Rerum Publicarum Sovieticarum Socialisticarum, series 1, Flora et Systematica Plantae Vasculares* 13: 173–232.

CHASE, M. K., D. E. SOLTIS, R. G. OLMSTEAD, D. MORGAN, D. H. LES, B. R. MISCHLER, M. R. DUVALL, R. A. PRICE, H. G. HILLIS, Y.-L. QIU, K. A. KRON, J. H. RETTIG, E. CONTI, J. D. PALMER, J. R. MANHART, K. J. SYTSMA, H. J. MICHAELS, W. J. KRESS, K. G. KAROL, W. D. CLARK, M. HEDRÉN, B. S. GAUT, R. K. JANSEN, K.-J. KIM, C. F. WIMPEE, J. F. SMITH, G. R. FURNIE, S. H. STRAUSS, Q.-Y. XIANG, G. M. PLUNKETT, P. S. SOLTIS, S. M. SWENSEN, S. E. WILLIAMS, P. A. GADEK, C. J. QUINN, L. E. EQUIARTE, E. GOLENBERG, G. H. LEARN JR., S. W. GRAHAM, S. C. H. BARRETT, S. DAYANANDAN, AND V. A. ALBERT. 1993. Phylogenetics of seed plants: an analysis of nucleotide sequences from the plastid gene *rbc*L. *Annals of the Missouri Botanical Garden* 80: 528–580.

CRONQUIST, A. 1981. An integrated system of classification of flowering plants. Columbia University Press, New York, New York, USA.

DOWELD, A. B. 1998. Carpology, seed anatomy and taxonomic relationships of *Tetracentron* (Tetracentraceae) and *Trochodendron* (Trochodendraceae). *Annals of Botany* 82: 413–443.

EFE, A. 1987. *Liquidambar orientalis* Mill. (sigla agaci) in morfolojik ve palinolojik ozellikleri uzerine arastirmalar. [Studies on the morphological and palynological characteristics of *Liquidambar orientalis* Mill. in Turkey]. *Istanbul Üniversitesi Orman Fakültesi Dergesi, series A* 37: 84–114.

ENDRESS, P. K. 1967. Systematische Studie über die verwandtschaftlichen Beziehungen zwischen den Hamameliaceen und Betulaceen. *Botanische Jahrbücher für Systematik, Pflanzengeschichte und Pflanzengeographie* 100: 249–317.

ENDRESS, P. K. 1989a. A suprageneric taxonomic classification of the Hamamelidaceae. *Taxon* 38: 371–376.

ENDRESS, P. K. 1989b. Aspects of evolutionary differentiation of the Hamamelidaceae and the lower Hamamelididae. *Plant Systematics and Evolution* 162: 193–211.

ENDRESS, P. K. 1989c. Phylogenetic relationships in the Hamamelidoideae. *In* P. R. Crane and S. Blackmore [eds.], Evolution, systematics, and fossil history of the Hamamelidae, vol. 1, 227–248. Systematics Association Special Volume No. 40A, Clarendon Press, Oxford, UK.

ENDRESS, P. K. 1993. Hamamelidaceae. *In* K. Kubitzki [ed.], The families and genera of vascular plants, vol. 2, 322–331. Springer-Verlag, New York, New York, USA.

ENDRESS, P. K., AND S. STUMPF. 1990. The diversity of stamen structures in 'Lower' Rosidae (Rosales, Fabales, Proteales, Sapindales). *Botanical Journal of the Linnean Society* 107: 217–293.

ENDRESS, P. K., AND A. IGERSHEIM. 1999. Gynoecium diversity and systematics of the basal eudicots. *Botanical Journal of the Linnean Society* 130: 305–393.

ESAU, K. 1965. Plant anatomy, 2nd ed. Wiley, New York, New York, USA.

FARRIS, J. S., M. KÄLLERSJÖ, A. G. KLUGE, AND C. BULT. 1995. Testing significance of incongruence. *Cladistics* 10: 315–319.

FELSENSTEIN, J. 1985. Confidence limits on phylogenies: an approach using the bootstrap. *Evolution* 39: 783–791.

FERGUSON, D. K. 1989. A survey of the *Liquidambaroideae* (Hamamelidaceae) with a view to elucidating its fossil record. *In* P. R. Crane and S. Blackmore [eds.], Evolution, systematics, and fossil history of the Hamamelidae, vol. 1, 249–272. Systematics Association Special Volume No. 40A, Clarendon Press, Oxford, UK.

GIFFORD, E. M., AND A. S. FOSTER. 1989. Morphology and evolution of vascular plants. W. H. Freeman, New York, New York, USA.

GOLDBLATT, P., AND P. K. ENDRESS. 1977. Cytology and evolution in the Hamamelidaceae. *Journal of the Arnold Arboretum* 58: 67–71.

GRAHAM, A. 1999. Late Cretaceous and Cenozoic history of North American vegetation. Oxford University Press, Oxford, UK.

GREGOR, H.-J. 1978. Die Miozänen Frucht- und Samen-Floren der Oberpfälzer Braunkohle I. Funde aus den sandigen Zwischenmitteln. *Palaeontographica* 167B: 8–103.

GUILLAUMIN, A. 1920. Hamamelidacées. *In* H. Lecomte [ed.], Flore Générale de l'Indochine, vol. 2. Masson et Cie, Paris, France.

HARMS, H. 1930. Hamamelidaceae. *In* A. Engler and K. Prantl [eds.], Die natürlichen Pflanzenfamilien, 2nd ed. vol. 18a, 303–343. Engelmann, Leipzig, Germany.

HOEY, M. T., AND C. R. PARKS. 1991. Isozyme divergence between eastern Asian, North American, and Turkish species of *Liquidambar* (Hamamelidaceae). *American Journal of Botany* 78: 938–947.

HOEY, M. T., AND C. R. PARKS. 1994. Genetic divergence in *Liquidambar styraciflua, L. formosana*, and *L. acalycina* (Hamamelidaceae). *Systematic Botany* 19: 308–316.

HUELSENBECK, J. P., AND F. R. RONQUIST. 2001. MrBayes: Bayesian inference of phylogenetic trees. *Bioinformatics* 17: 754–754.

HUFFORD, L. 1992. Rosidae and their relationships to other non-magnoliid dicotyledons: a phylogenetic analysis using morphological and chemical data. *Annals of the Missouri Botanical Garden* 79: 218–248.

HUFFORD, L., AND P. R. CRANE. 1989. A preliminary phylogenetic analysis of the 'lower' Hamamelidae. *In* P. R. Crane and S. Blackmore [eds.], Evolution, systematics, and fossil history of the Hamamelidae, vol. 1,

175–192. Systematics Association Special Volume No. 40A, Clarendon Press, Oxford, UK.

HUFFORD, L., AND P. K. ENDRESS. 1989. The diversity of anther structures and dehiscence patterns among Hamamelididae. *Botanical Journal of the Linnean Society* 99: 301–346.

ICKERT-BOND, S. M., K. B. PIGG, AND J. WEN. 2004. Resolving phylogeny within the family Altingiaceae: implications from anatomy of infructescences and molecular data sets. Botany 2004, annual meeting of the Botanical Society of America, Snowbird, Utah, USA, abstract 690. Available at website, http://www.2004.botanyconference.org/engine/search/index.php?func=detail&aid=690.

JUDD, W. S., C. S. CAMPBELL, E. A. KELLOGG, P. F. STEVENS, AND M. J. DONOGHUE. 2002. Plant systematics. A phylogenetic approach, 2nd ed. Sinauer, Sunderland, Massachusetts, USA.

KALSHOVEN, G. E. 1937. The pest and blights of the Rasamala tree. *Tectona* 30: 162–176.

KAPLAN, D. R. 1984. The concept of homology and its central role in the elucidation of plant systematic relationships. *In* T. Duncan and T. F. Stuessy [eds.], Cladistics: perspectives on the reconstruction of evolutionary history, 51–70. Columbia University Press, New York, New York, USA.

KAUL, U., AND R. N. KAPIL. 1974. *Exbucklandia populnea*—from flower to fruit. *Phytomophology* 24: 217–228.

LI, J., A. L. BOGLE, AND A. S. KLEIN. 1997a. Interspecific relationships and genetic divergence of the disjunct genus *Liquidambar* (Hamamelidaceae) inferred from DNA sequences of plastid gene matK. *Rhodora* 99: 229–240.

LI, J., A. L. BOGLE, AND A. S. KLEIN. 1997b. Phylogenetic relationships of the Hamamelidaceae inferred from sequences of internal transcribed spacers (ITS) of nuclear ribosomal DNA. *American Journal of Botany* 86: 1027–1037.

LI, J., AND M. J. DONOGHUE. 1999. More molecular evidence for interspecific relationships in *Liquidambar* (Hamamelidaceae). *Rhodora* 101: 87–91.

LITTLE, E. L. 1971. Atlas of United States trees, vol. 1, Conifers and important hardwoods. U. S. Department of Agriculture, Forest Service, Miscellaneous Publication No. 1146, United States Government Printing Office, Washington, D.C., USA.

LOBOVA, T. A., A. M. SCOTT, F. BLANCHARD, H. PECKHAM, AND P. CHARLES-DOMINIQUE. 2003. *Cecropia* as a food resource for bats in French Guiana and the significance of fruit structure in seed dispersal and longevity. *American Journal of Botany* 90: 388–403.

MADDISON, D. R., AND W. P. MADDISON. 2000. MacClade: analysis of phylogeny and character evolution. Sinauer, Sunderland, Massachusetts, USA.

MAGALLÓN, S., P. R. CRANE, AND P. S. HERENDEEN. 1999. Phylogenetic pattern, diversity, and diversification of eudicots. *Annals of the Missouri Botanical Garden* 86: 297–372.

MAI, D. H. 1968. Zwei ausgestorbene Gattungen im Tertiär Europas und ihre Florengeschichtliche Bedeutung. *Palaeontographica* 123B: 184–199.

MEIKLE, R. D. 1977. Flora of Cyprus, vol. 1. Betham-Moxum Trust, Royal Botanic Gardens, Kew, UK.

MELIKIAN, A. P. 1971. The anatomical structure of the spermoderm of the representatives of the genera *Liquidambar* L. and *Altingia* Nor. relative to its systematics. *Biologicheski Zhurnal Armenii* 24: 50–55.

MELIKIAN, A. P. 1973. Seed coat types of Hamamelidaceae and allied families in relation to their systematics. *Botaneski Zhurnal* 58: 350–359.

MIONE, T., AND A. L. BOGLE. 1990. Comparative ontogeny of the inflorescence and flower of *Hamamelis virginiana* and *Loropetalum chinense* (Hamamelidaceae). *American Journal of Botany* 77: 77–91.

PARKS, C. R., AND J. F. WENDEL. 1990. Molecular divergence between Asian and North American species of *Liriodendron* (Magnoliaceae) with implications of fossil floras. *American Journal of Botany* 77: 1243–1256.

PIGG, K. B., S. M. ICKERT-BOND, AND J. WEN. 2004. Anatomically preserved *Liquidambar* (Altingiaceae) from the middle Miocene of Yakima Canyon, Washingon state, USA, and its biogeographic implications. *American Journal of Botany* 91: 499–509.

POSADA, D., AND K. A. CRANDALL. 1998. MODELTEST: testing the model of DNA substitution. *Bioinformatics* 14: 817–818.

QUI, Y.-L., M. W. CHASE, AND C. R. PARKS. 1995. A chloroplast DNA phylogenetic study of the eastern Asia-eastern North America disjunct section *Rytidospermum* of *Magnolia* (Magnoliaceae). *American Journal of Botany* 82: 1582–1588.

QUI, Y.-L., M. CHASE, S. HOOT, E. CONTI, P. R. CRANE, K. J. SYTSMA, AND C. R. PARKS. 1998. Phylogenetics of the Hamamelidae and their allies: parsimony analyses of nucleotide sequences of the plastid gene *rbc*L. *International Journal of Plant Sciences* 159: 891–905.

RAO, R. P. M. 1974. Seed anatomy in some Hamamelidaceae and phylogeny. *Phytomorphology* 24: 113–139.

REICHINGER, K. H. 1943. Flora Aegaea. Flora der Inseln und Halbinseln des Ägäischen Meeres. *Akademie der Wissenschaften in Wien. Mathematisch-Naturwissenschaftliche Klasse. Denkschriften* 105: 1–924.

REINSCH, A. 1890. Über die anatomischen Verhältnisse der Hamamelidaceae mit Rücksicht auf ihre systematische Gruppierungen. *Botanische Jahrbücher für Systematik* 11: 347–395.

SCHMITT, D. 1965. The pistillate inflorescence of sweet-gum (*L. styraciflua*). *Silvae Genetica* 15: 33–35.

SHI, S. Y., H.-T. CHANG, Y. CHEN, L. QU, AND J. WEN. 1998. Phylogeny of the Hamamelidaceae based on the ITS sequences of nuclear ribosomal DNA. *Biochemical Systematics and Ecology* 26: 55–69.

SHI, S., Y. HUANG, Y. ZHONG, Y. DU, Q. ZHANG, H. CHANG, AND D. E. BOUFFORD. 2001. Phylogeny of the Altingiaceae based on cpDNA *mat*K, PY-IGS and nrDNA ITS sequences. *Plant Systematics and Evolution* 230: 13–24.

SHOEMAKER, D. N. 1905. On the development of *Hamamelis virginiana*. *Botanical Gazette* 39: 248–266.

SOLTIS, D. E., P. S. SOLTIS, M. W. CHASE, M. E. MORT, D. C. ALBACH, M. ZANIS, V. SAVOLAINEN, W. H. HAHN, S. B. HOOT, M. F. FAY, M. AXTELL, S. M. SWENSEN, L. M. PRINCE, W. J. KRESS, K. C. NIXON, AND J. S. FARRIS. 2000. Angiosperm phylogeny inferred from 18S rDNA, *rbc*L, and *atp*B sequences. *Botanical Journal of the Linnean Society* 133: 381–461.

SWOFFORD, D. I. 2002. PAUP*: phylogenetic analysis using parsimony (*and other methods), version 4. Sinauer, Sunderland, Massachusetts, USA.

TARDIEU-BLOT, M. L. 1965. Hamamelidaceae. *In* A. Aubréville and M. L. Tardieu-Blot [eds.], Flore du Cambodge du Laos et du Viêtnam, fascicle 4, 75–116. Muséum National d'Histoire Naturelle, Paris, France.

TEMPLETON, A. R. 1983. Phylogenetic inference from restriction endonuclease cleavage site maps with particular reference to the evolution of humans and the apes. *Evolution* 37: 221–244.

TIFFNEY, B. H. 1986. Fruit and seed dispersal and the evolution of the Hamamelidae. *Annals of the Missouri Botanical Garden* 73: 394–416.

TIFFNEY, B. H., AND S. R. MANCHESTER. 2001. The use of geological and paleontological evidence in evaluating plant phylogeographic hypotheses in the northern hemisphere Tertiary. *International Journal of Plant Sciences* 162: S3–S17.

TONG, K. 1930. Studien über die Familie der Hamamelidaceae, mit besonderer Berücksichtigung der Systematik und Entwicklungsgeschichte von *Corylopsis*. *Bulletin of the Department of Biology Sun Yatsen University* 2.

VINK, W. 1957. Hamamelidaceae. *In* C. G. G. J. van Steenis [ed.], Flora Malesiana, vol. 5, 363–379. Nationaal Herbarium Nederland, Universiteit Leiden branch, Leiden, Netherlands.

WEN, J. 1998. Evolution of the eastern Asian and eastern North American disjunct pattern: insights from phylogenetic studies. *Korean Journal of Plant Taxonomy* 28: 63–81.

WEN, J. 1999. Evolution of eastern Asian and eastern North American disjunct distributions in flowering plants. *Annual Review of Ecology and Systematics* 30: 421–455.

WEN, J. 2001. Evolution of eastern Asian-eastern North American biogeographic disjunctions: a few additional issues. *International Journal of Plant Sciences* 162: S117–S122.

WILLIAMS, J. 1855. Amentaceae. *In* J. H. Balfour [ed.], A manual of botany: being an introduction to the study of the structure, physiology, and classification of plants, 3rd ed., 524. Griffin, London, UK.

WILSON, P. 1905. Altingiaceae. *In* N. L. Britton and L. M. Underwood [eds.], North American flora, vol. 22, 189. New York Botanical Garden, New York, New York, USA.

WISNIEWSKI, M., AND A. L. BOGLE. 1982. The ontogeny of the inflorescence and flower of *Liquidambar styraciflua* L. (Hamamelidaceae). *American Journal of Botany* 69: 1612–1624.

WOOD, C. E. JR. 1972. Morphology and phytogeography: the classical approach to the study of disjunctions. *Annals of the Missouri Botanical Garden* 59: 107–124.

ZHANG, Z.-Y., AND J. WEN. 1996. The seed morphology in Hamamelidaceae and its systematic evaluation. *Acta Phytotaxonomica Sinica* 34: 538–546.

ZHANG, Z. Y., H. T. ZHANG, AND P. K. ENDRESS. 2003. Hamamelidaceae. *In*

Z.-Y. Wu, P. H. Raven, and D.-Y. Hong [eds.], Flora of China, vol. 9, 18–42. Science Press, Beijing, China.

ZHOU, Z.-K., W. L. CREPET, AND K. C. NIXON. 2001. The earliest fossil evidence of the Hamamelidaceae: Late Cretaceous (Turonian) inflorescences and fruits of Altingioideae. *American Journal of Botany* 88: 753–766.

APPENDIX. Voucher specimens of *Liquidambar* studied.

Taxon. *Collector*, locality.

Liquidambar L., **section *Liquidambar*** Harms. ***L. acalycina*** Hung T. Chang. *Sino-American Exped. No. 1660* (A), China: Guizhou, Yinjiang Xian, between Zhangjiaba and Huguoshi. *Sino-American Exped. No. 1758* (A), China: Guizhou, Yinjiang Xian, vicinity of Xiapingsho. *Sino-American Exped. No. 1950* (A), China: Hubei, Metasequioa Region of Lichuan Xian. *A.L. Bogle 1568* (ASU), USA: Massachusetts, Arnold Arboretum, cult. *J.L. Gressitt 2415* (A), China: Hubei, vicinity of Shui-sa-pa. *C. Wang 44102* (MO), China: Guangdong, Ruyuan Xian. *E.H. Wilson 513, 518* (A), China: Hubei. *E.H. Wilson 513* (GH), China: Hubei. *K. Yao 11486* (A), China: Jiangxi, De-xin county. *S.-L. Zhou 9908* (ASU), China: Zhejiang.

L. orientalis Miller. *A.L. Bogle 1561* (ASU), USA: Washington, University of Washington Arboretum, cult. *K. Boratynska et al. 15* (K), Greece: Rhodes Island, SE of Salakos. *K. Boratynska* et al. *164* (K), Greece: Rhodes Island, between Malona and Archangelos. *P.H. Davis 40317* (K), Greece: Rhodes Island, Salakos. *P.H. Davis 13474* (E), Turkey: Mughla near Dogusbelen. *Danish Bot. Trans-Asia Expedition III, No. 2081* (E), Turkey: Köycegiz. *A. Fiori 230* (FI), Greece: Rhodes Island, Convento d'Iskiati. *A. Fiori 231* (FI), Greece: Rhodes Island, Saduras. *A. Fiori* s.n. (FI), Italy, Rome, cult. *R.C. Hitchin* s.n. (F), USA: Washington, University of Washington Arboretum, cult. *G. Jannone* (FI), Greece: Rhodes Island, near Severagno. *Khan et al. 45* (E), Turkey: Mugla, Marmaris, Erküs. *E. Martinetto* s.n. (ASU), Italy: Rome, cult. *E. Murray 1020* (A), Turkey: Mulga, Paludal place 1 km NE of Marmaris.

L. styraciflua L. *A.L. Bogle 1565* (ASU), USA: Oregon, Eugene, cult. *A.L. Bogle 1566* (ASU), USA: Oregon, Eugene, University of Oregon campus, cult. *A.L. Bogle 1567* (ASU), USA: Massachusetts, Arnold Arboretum, cult. *G.L. Bracewell 42* (MO), USA: Georgia, Laurens Co., 1/2 mi S of Brewton. *C. Christy* s.n. (ASU), USA: Georgia, Richmond Co., Augusta. *T.B. Croat 25056* (MO), USA: Florida, Alachua Co., Gainesville, vicinity of Lake Alice. *L. Hubricht B-1357* (MO), USA: Arkansas, Newton Co., Ponca. *S.M. Ickert-Bond* s.n. (ASU), USA: Illinois, Clark Co., Hyde Park, cult. *S.M. Ickert-Bond 1383* (F), Mexico: Hidalgo, Mineral del Monte. *S.M. Ickert-Bond 1390* (F), Mexico: Veracruz, Banderilla. *S.M. Ickert-Bond 1391* (F), Mexico: Veracruz, Cascada del Texolo. *S.M. Ickert-Bond 1394* (F), Mexico: Veracruz, Coscomatepec. *C.J. Leyva 613* (MO), Mexico: Hidalgo, Medio Monte. *M. Nee 23457a* (F), Mexico: Veracruz, Jardin Botanica Javier Clavijero. *E.J. Palmer 17478* (F), USA: Tennessee, Haywood Co., near Shepherd. *K.B. Pigg* s.n. (ASU), USA: Ohio, Franklin Co., Columbus. *E. & M. Sundell 653* (ASU), USA: Louisiana, New Orleans, cult. *R.D. Thomas 205* (ASU), USA: Louisiana, US 80 W of LA 546. *D.A. Young* s.n. (ASU), USA: California, Marin Co., cult.

Liquidambar L., **section *Cathayambar*** Harms. ***L. formosana*** Hance. *G. Hao 922* (ASU), China: Guangdong. *Hu 6593* (ASU), China: Hong Kong, marketplace, cult. *S.M. Ickert-Bond 1260* (F), China: Hong Kong, New Territories, Shing Mun Country Park. *S.M. Ickert-Bond 1328* (F), China: Jiangxi, Long Nan Co., roadside. *S.M. Ickert-Bond 1347* (F), China: Guangdong, Heping Co., Li Yuan. *S.M. Ickert-Bond 1375* (F), China: Zhejiang, Qingyuan Co., Wulingkeng village, near river. *D.A. Keil K13781* (ASU), USA: California, San Bernardino Co., cult. *F.G. Meyer 14425* (ASU, F), USA: Georgia, University of Georgia, Athens, Clarke Co., cult. *F.G. Meyer 15047* (ASU), USA: Washington D.C., USSR embassy, cult. *W.T. Tsang 23613* (GH), China: Hunan, P'ing T'ou Shan, T'ang Wan village, Yi Chang district. *S.-L. Zhou 9907* (F), China: Guangdong, Guangzhou, South China Botanical Garden.